UNIVERSIDAD DE CHILE
FACULTAD DE CIENCIAS FÍSICAS Y MATEMÁTICAS
DEPARTAMENTO DE INGENIERÍA QUÍMICA, BIOTECNOLOGÍA Y MATERIALES

DEVELOPMENT OF A METHOD FOR PLANNING A RESILIENT MULTI-VECTOR ENERGY SYSTEM THROUGH A MULTI-OBJECTIVE OPTIMIZATION MODEL

TESIS PARA OPTAR AL GRADO DE MAGÍSTER EN CIENCIAS DE LA INGENIERÍA, MENCIÓN QUÍMICA

MEMORIA PARA OPTAR AL TÍTULO DE INGENIERA CIVIL QUÍMICA

GABRIELA ALEJANDRA VERA HOFMANN

PROFESOR GUÍA:
FELIPE DÍAZ ALVARADO

PROFESOR CO-GUÍA:
JANNIK HAAS

MIEMBROS DE LA COMISIÓN:
JUAN ASENJO DE LEUZE
SIMÓN MORENO LEIVA
J CRISTIAN SALGADO HERRERA

SANTIAGO DE CHILE
2020

Summary

RESUMEN DE LA TESIS PARA OPTAR AL TÍTULO DE:
INGENIERA CIVIL QUÍMICA Y GRADO DE MAGÍSTER EN CIENCIAS DE LA INGENIERÍA, MENCIÓN QUÍMICA
POR: GABRIELA ALEJANDRA VERA HOFMANN
FECHA: 17/01/2020
PROFESOR GUÍA: FELIPE DÍAZ ALVARADO

DEVELOPMENT OF A METHOD FOR PLANNING A RESILIENT MULTI-VECTOR ENERGY SYSTEM THROUGH A MULTI-OBJECTIVE OPTIMIZATION MODEL

The operation of energy systems is affected by natural disasters; however, these systems can be improved if their resilience to such events is taken into account at the design phase. Moreover, the use of renewable energy technologies is increasing, but they are highly variable since they depend on climate conditions. Thus, coupling energy sectors using multi-energy systems has proven to be beneficial in smoothing out the variability of renewable sources; nonetheless, the impact of natural disasters on these systems has not been thoroughly studied. The literature review has shown a lack in the study of resilience metrics for energy systems, specifically, there is no study observed for multi-energy systems. Therefore, the goal of this thesis is to develop a method to optimally plan a multi-energy system including resilience in its design.

This method includes three stages: i) investment planning of a multi-energy system with two targets: resilience and costs, the first one being a core-part of our work: we create a new resilience indicator, ii) operational simulation of the system in case of a disrupting event, and iii) the index validation where we consider the uncertainty of restoration time through a Monte Carlo simulation. Both simulations are iterative processes, in which we compare the results with the predicted resilience value in the planning stage. If the results differ, the methodology is repeated, modifying the resilience index to obtain an appropriated one.

The results of the planning stage show a clear trade-off between both targets, where increasing resilience involves an increase in costs. The operational simulation of the system in case of an event shows a higher value of resilience than predicted by the indicator because the model is free to adapt the power delivered, minimizing the unserved energy. To validate the model, we performed a Monte Carlo simulation. It shows lower results than predicted due to the restoration function used. Even though the values are lower than predicted, the increase in resilience is expected; therefore, the method looks promising to plan a multi-energy system including resilience.

Resumen

RESUMEN DE LA TESIS PARA OPTAR AL TÍTULO DE:
INGENIERA CIVIL QUÍMICA Y GRADO DE MAGÍSTER EN CIENCIAS DE LA INGENIERÍA, MENCIÓN QUÍMICA
POR: GABRIELA ALEJANDRA VERA HOFMANN
FECHA: 17/01/2020
PROFESOR GUÍA: FELIPE DÍAZ ALVARADO

DESARROLLO DE UN MÉTODO PARA EL DISEÑO DE UN SISTEMA MULTI-ENERGÍA RESILIENTE MEDIANTE UN MODELO DE OPTIMIZACIÓN MULTI-OBJETIVO

Uno de los grandes problemas de la operación de sistemas energéticos es la ocurrencia de desastres naturales. Esto se podría mejorar si se considera la resiliencia en su etapa de diseño. Además, el uso de energías renovables está aumentando, pero estas son altamente variables, al depender de las condiciones climáticas. Es por esto, que la integración de los distintos sectores energéticos, usando sistemas multi-energéticos, ha demostrado traer beneficios minimizando esta variabilidad. Sin embargo, el impacto de desastres naturales en estos sistemas no ha sido estudiado en detalle. La bibliografía muestra una falta en el estudio de métricas de resiliencia en sistemas energéticos y menos para sistemas multi-energéticos. Es por esto, que el objetivo de esta tesis es desarrollar un método para planificar óptimamente un sistema multi-energético incluyendo resiliencia en el diseño.

Este método se divide en tres etapas, primero, i) la planificación de la inversión de un sistema multi-energético con dos objetivos: minimizar costos y maximizar la resiliencia, siendo este último parte esencial de este trabajo, ya que se propone un nuevo indicador de resiliencia; ii) la simulación operacional del sistema dado un evento disruptivo; y iii) la validación del indicador de resiliencia, donde se considera la incertidumbre del tiempo de recuperación de las distintas tecnologías, a través de una simulación de Montecarlo. Ambas simulaciones son procesos iterativos, donde se compara el valor de resiliencia obtenido con el que se predijo en la etapa de planificación. Si los resultados difieren, se repite la metodología modificando el indicador de resiliencia hasta obtener uno apropiado.

Los resultados de la etapa de planificación muestran una contraposición de ambas funciones objetivo, donde aumentar la resiliencia del sistema conlleva mayores costos. La simulación de la operación del sistema muestra valores superiores a los esperados de la etapa de planificación, porque, a diferencia de la planificación, en esta etapa el modelo es libre de adaptar sus flujos minimizando la energía no suministrada. La validación del modelo con la simulación de Montecarlo muestra valores menores a los esperados, lo que se explica por la diferencia de las funciones de recuperación de las tecnologías. A pesar de que con este método los valores son inferiores a los que predice el modelo en la etapa de planificación, el comportamiento de aumentar la resiliencia es el esperado, por lo que el método es prometedor para planificar un sistema multi-energético con resiliencia.

Agradecimientos

Primero agradecer a mi comisión, especialmente a Felipe, Jannik y Simón. Felipe, gracias por ser mi guía en la tesis y durante la carrera, por enseñarme a ser más ordenada y por las oportunidades que surgieron por trabajar contigo durante la carrera. Jannik y Simón, gracias por recibirme en Alemania, por todo el apoyo que me dieron trabajando allá y el que siguió estando en Chile.

Gracias a mi familia, porque gran parte de este logro se los debo a ustedes, por apoyarme en cada decisión que tomé a lo largo de la vida. A mis papas por estar orgullosos de cada logro preguntarme día a día como iba la tesis y escucharme aun cuando no entendían mucho. Javier, gracias por todo el apoyo, siempre fuiste el más exigente conmigo porque sabías lo que podía lograr.

A mis perros que me acompañaron durante mi vida universitaria. Kai por acompañarme en cada noche de estudio en plan común y Roy por ser mi compañero incondicional en cada paseo juntos y lo que me hacía dejar de trabajar y llegar a mi casa.

Gracias Cahuate por tu eterna amistad, por estar conmigo en cada pasito de mi vida y por mantener nuestra amistad incluso habiendo tomado otros caminos.

Nicole, gracias por todos estos años de amistad, por los almuerzos eternos en la U que me sacaban un rato de mi estudio y por los viajes que hicimos y los que vendrán.

Gene, gracias por estar conmigo desde plan común, por estar siempre ahí para lo que necesitara con tus buenas vibras.

Gracias a mis compañeros de taller Dani, Panchi y Nico, porque cada momento de trabajo y estrés eran mejores con ustedes. Con ustedes aprendí mucho más de lo que la U me podía enseñar.

A mi grupo de amigos de IQBT: Pancho, Nefta, Benja P., Benja C., Juampa, Cami, Checo y Rafa. Mi paso por IQBT no hubiera sido lo mismo sin ustedes. Gracias por todos los momentos compartidos.

Willy, gracias por perder el tiempo conmigo cuando necesitaba un descanso de mi estudio. Gracias por todo lo que me ayudaste académicamente, por lo mucho que aprendí contigo y sigo aprendiendo.

Gracias a mis amigas de volley: Nacha, Shtef, Jenny, Vale, Gabi, Connie y Nati, por ser mi desconexión del estudio por tantos años y por ser mucho más que parte de un equipo.

Y por último agradecer a todas las personas que de alguna forma me acompañaron en este proceso y aportaron, aunque sea con un granito de arena a mi desarrollo personal y profesional.

Contents

Figures Index

Tables Index

1. Chapter 1: Introduction

1.1 Motivation and Theoretical Framework

The growth of electricity demand and the need to mitigate climate change demand the use of renewable energies [1]. For reaching high-shares of renewables, coupling different energy sectors has proven to be beneficial in smoothing out the variability of renewable sources (e.g. photovoltaics PV) [2]. These systems allow us to identify many readily available options and synergies. Therefore, tools for a systematic design of these systems are crucial for helping the decision-makers in this task.

Multi-energy systems (MES) consist in a system whereby different energy vectors, like electricity, heat, cooling, fuels, and transport interact with each other at various levels. MES represent an important opportunity to increase economic and environmental performance compared to classical energy systems whose sectors are treated separately [3].

MES, like any other system, are vulnerable to the effects of earthquakes, which may result in significant disruption of power supply [4]. If a MES is planned considering disruptions as a possibility, the system can be designed to reduce negative consequences.

Hence, it is important to take resilience into account in their design. Resilience is a term widely used in multiple disciplines, including psychology, ecology, environmental science, among others. The multidisciplinary use of resilience implies the ability of an entity or system to return to its normal state after a disruption [5].

The *resilience curve* is used to graphically represent resilience. This curve represents the system's health over time [6], as shown in Fig. 1. In the beginning, the system is in steady-state with the health Q_0. Nonetheless, in time t_0, an event occurs, which causes a reduction in the system's health, reaching the value Q_e. After the event, the system starts a recovery state, until it reaches the steady state again in time t_{rec}.

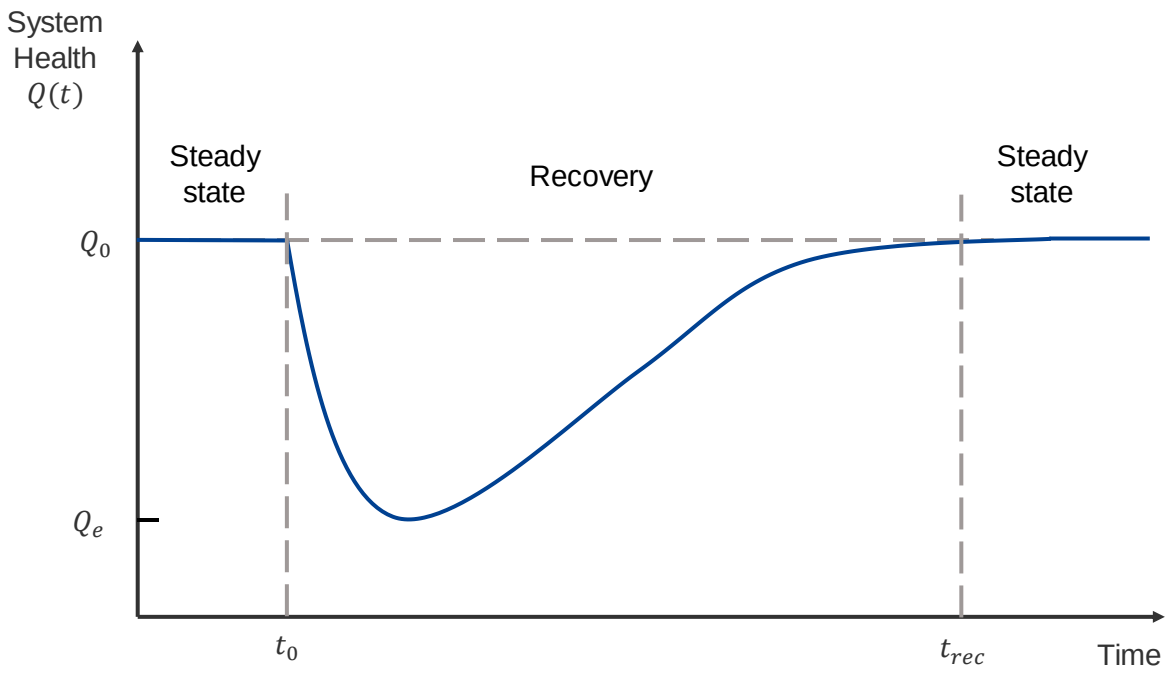

Fig. 1: Graphic representation of a resilience curve.

For a system to be resilient, it should have the following characteristics (or *dimensions*): (i) Robustness: the ability of systems to withstand a given level of stress without suffering degradation. (ii) Redundancy: the extent to which systems are substitutable and can satisfy functional requirements in the event of disruption. (iii) Resourcefulness: the capacity to apply material and human resources to meet established priorities and achieve goals. (iv) Rapidity: the capacity to meet priorities and achieve goals in a timely manner to contain losses [7].

To consider resilience in the systems it is important to predict their behavior in the event of an earthquake. Therefore, two main concepts are used: fragility curve and restoration curve. The former describes the probability of reaching or exceeding a damaged state, while the latter describes the health of the system over time [4].

Considering resilience when planning energy systems is important in order to reduce disruptions. Some authors have studied different ways to measure resilience, proposing metrics for different application areas [7, 8]. Literature reveals that there are multiple ways to describe the concept; however, some authors agree on the recovery ability. Despite resilience is widely studied, a resilience indicator for coupled multi-energy systems has not been observed. As a consequence, this study aims at filling this gap, developing a resilience indicator for MES.

On the other hand, there is much recent work on designing multi-energy systems [3] whose most common goal is to minimize the costs of the system. In fact, even some environmental indexes have been included in these formulations [9].

Incorporating resilience in the planning stage of other systems, such as water resources, has shown adverse consequences on costs and environmental aspects as the redundancy of the system increases [10][11]. This implies that is important to consider the impact of planning with resilience.

Other authors have studied how to incorporate resilience in power systems optimization. For example, [12] described and applied a resilience assessment and an adaptation framework of a power system exposed to seismic events. This framework optimally configures the network operation and restoration [12]. Moreover, [13] proposed an optimization framework for designing resilient power grids against natural hazards to make optimal decisions on network investment [13]. Nevertheless, planning a multi-energy system with a resilience target has not been observed. Therefore, the framework we propose aims at filling this gap by planning a multi-energy system.

1.2 Research Questions and Goals

The main goal of this thesis is to develop a method to optimally plan a multi-energy system including resilience in its design. More precisely, this study answers the following questions:

- RQ1: How to measure resilience?
- RQ2: How to simulate the resilience of a multi-energy system given a certain disturbance?
- RQ3: How to endogenize this resilience index in a multi-energy system expansion model?
- RQ4: What is the impact of planning considering resilience at the design phase on investment costs in an applied case?

To answer each research question and reach the main goal, this thesis has the following specific goals:

- SG1: To provide a comprehensive review of the academic literature, focused on different resilience metrics.
- SG2: To simulate resilience of a multi-energy system in the event of a disturbance.
- SG3: To propose a new resilience indicator for multi-energy systems.
- SG4: To plan investment and make operational decisions in an applied case using the proposed indicator and an economic indicator through a multi-objective optimization model.

This thesis has two novelties. The first one is the method for planning a MES considering resilience and costs through multi-objective optimization. The second one is the resilience indicator used, which is analog to the loss of energy expectation (LOEE) in power systems but extended to MES.

The present thesis consists of 7 main chapters: i) Introduction: where the motivation and the theoretical framework as well as the research questions and goals are exposed. ii)

Methodology: we propose a framework to plan a multi-energy system taking resilience into account. It consists of three stages: investment planning, operational simulation and resilience index validation. In addition, we present the optimization model used, the superstructure and the optimization problem, and our case study. iii) Resilience metrics: we review different resilience metrics from literature and we adapt one for this study; iv) Operational simulation and resilience measurement: we use this metric to quantify resilience through an operational simulation. This chapter is important to develop a new resilience indicator to use the resilience value as a reference in the following stage. v) Development of a new resilience indicator for the system design: based on the previous chapter, we develop a new resilience indicator to design a multi-energy system. vi) Planning of a resilient and low-cost multi-energy system: using the previous work, we use the proposed framework to plan a multi-energy system considering resilience in its design. vii) Conclusions: finally, we mention some important conclusions related to our research.

2. Chapter 2: Methodology

This chapter presents the thesis methodology. First, we propose a framework to plan a multi-energy system considering resilience. This framework is divided into stages: investment planning, operational simulation and resilience index validation, which are explained in detail. Then, we explain the optimization model used, the superstructure, and finally we describe our case study.

2.1 Framework

Incorporating a resilience index in a multi-objective optimization allows us to define relative importance to each goal and to study the trade-off between the functions. Therefore, we propose a framework that plans a multi-energy system considering a resilience target in its design and optimizes the network operation after being exposed to a hazard. This framework is divided into three main stages: investment planning, operational simulation, and resilience index (RI) validation, as presented in Fig. 2.

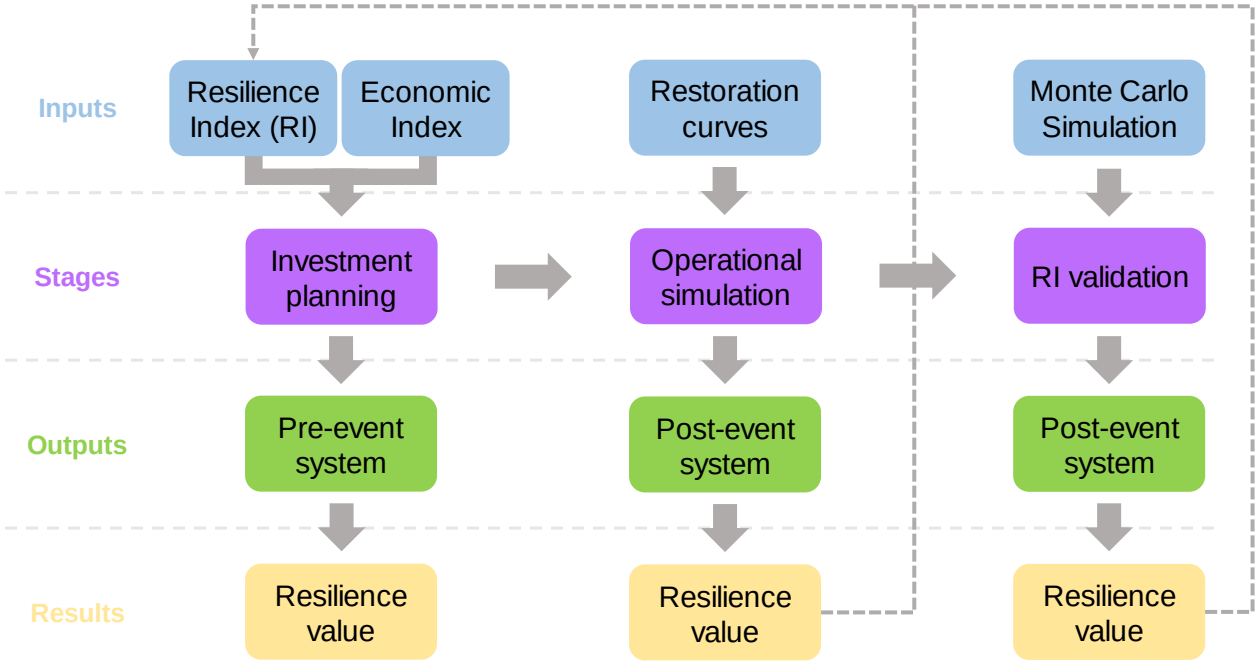

Fig. 2: Methodology of the proposed framework

To understand the state of the art of the different metrics already proposed we will provide a comprehensive review of the academic literature. In this review, we present some resilience metrics, analyze other metrics related to the topic, and finally adapt a metric for this study.

The first stage of the proposed framework is the investment planning, which consists in a multi-objective optimization to decide the capacity and operation of each component of the system. The optimization functions (OF) are economic and resilience indicators. The latter

OF is a core-part of our work: we create a resilience indicator capable of ensuring computational tractability. The output of the investment planning stage is the configuration of the pre-event system, which operates in normal conditions. Since we are planning with resilience, we also obtain as output an expected value of resilience from this stage.

When a hazard such as an earthquake occurs, some technologies may suffer damage (vulnerability). To predict the damage-state that each technology may reach, we use the HAZUS method (for more detail see Appendix A), to obtain their restoration curves, which describe the fraction of the system that is expected to be operational as a function of time following the earthquake. The incorporation of the damage-state of each technology implies a possible reduction in the capacities of the technologies, which might threaten the system's health (i.e. this might lead to unserved energy). To determine the best system configuration that minimizes the energy not supplied, we create an operational simulation. This simulation takes the restoration curve of each technology as input. The output of this stage is the post-event system behavior over time. From this behavior, we calculate resilience using the adapted metric from the literature review. This final resilience value is compared to the value from the previous stage, if they are different, we modify the resilience indicator and the methodology is repeated until an appropriated indicator is obtained.

The last stage of the framework is the validation of the resilience index used in the first stage. To do this, we perform a Monte Carlo Simulation (MCS) (for more detail see Appendix B) with the reposition time as a random variable, and its distribution is given from fragility curves. This value is then compared with the resilience value obtained from the previous stages. Like the previous stage, if the values are similar, the resilience index is accepted. Otherwise, the methodology is repeated, modifying the resilience index to obtain an appropriated one.

The iterative process presented in this framework is applied to the operational simulation stage. However, this thesis presents the final indicator obtained from the process. The iterative process is not performed in the last stage because of the duration of the study.

2.2 Optimization Model

To develop the abovementioned methodology, we use an optimization model. This model gives us the system operation based on different inputs. It is for MES and extends an existing energy planning tool, adapted from [14] and [34] and it is illustrated in Fig. 3. We adapted this model adding resilience as a new objective function (OF).

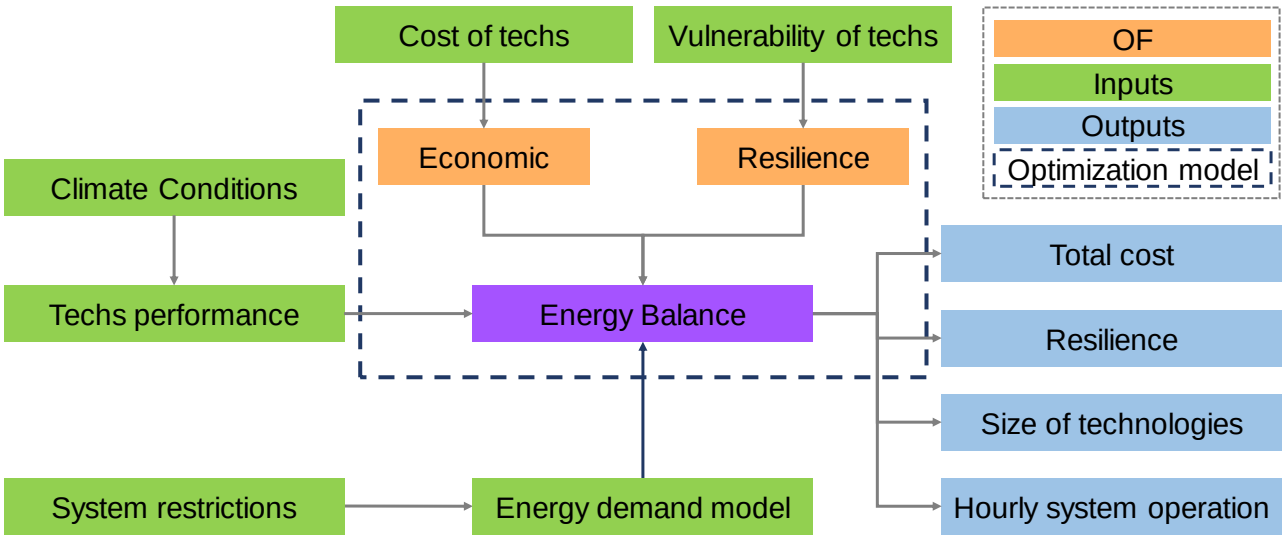

Fig. 3: Optimization model used. Adapted from [14] *and [34].*

The optimization model is based on energy balances and OFs, which needs parameters as inputs, and the output is the expected result of the system. The model is a multi-objective optimization problem (MOP) (for more detail see Appendix C). It uses two OFs: economic function and resilience. To quantify those targets, the model needs the cost and vulnerability (fragility curves and restoration curves) of each technology, respectively.

The model should help to decide which technology to install, the capacity and the configuration of the system. The model takes planning and operational decisions, and the final product is the optimal system design and its operation over time.

The optimization model is a linear programming problem (LP). To solve this model, we use the solver CPLEX in the computational program GAMS. The input and output data are managed with EXCEL, while the graphics are generated with MATLAB.

The complete model formulation, the inputs used for the model and the GAMS formulation are presented in Appendixes G, H and I, accordingly.

2.3 Superstructure

The superstructure used in this thesis describes a general fully-renewable multi-energy system, as shown in Fig. 4. This system has different types of technology: primary generation PG, transformation technologies TT (which transform one type of energy to another), storage S of the different energy types, and the process D which demands energy. We consider three types of energy: heat, fuel and electricity. Every energy type can be generated by different technologies (e.g. photovoltaics PV, wind turbine). The transformation of energy can also be addressed through different technologies (e.g. heat to fuel, electricity to heat, etc.). Every combination between input and output of the same energy type is possible.

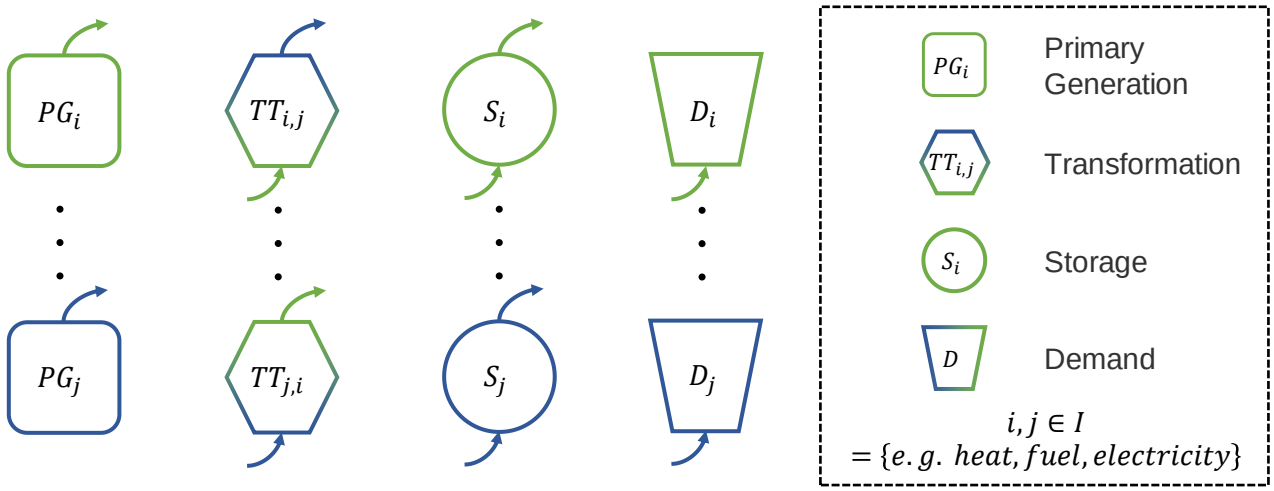

Fig. 4: Model superstructure.

The superstructure of the system is analog to a process, which has different units and connections. Therefore, we develop the model as a process with energy balances.

The complete nomenclature of the sets, parameters and variables used in this thesis are detailed in Section 8.

2.4 Case Study

To study the application of the proposed approach, we use the case study presented in Fig. 5. Specifically, it consists in a fully-renewable multi-energy system that supplies the energy demand for copper mining in Chile [13]. Mining demands energy in the form of electricity, fuels, and heat. It considers primary energy generation of electricity and heat, storage for all kinds of energy, and energy transformation technologies.

Primary energy generation considers wind power and three different solar energy technologies (photovoltaics, concentrated solar power CSP –parabolic trough- and flat plate solar-thermal collectors). For electricity storage, we use lithium batteries, for fuel storage hydrogen tanks, and for heat molten salts storage and hot water tanks. Transformation technologies consider CSP-power block to generate electricity from heat, fuel cells to transform fuel into electricity, electrolyzer which uses electricity to generate fuel, and heating rod to transform electricity into heat. The specific nomenclature used for this case study is described in Section 8.

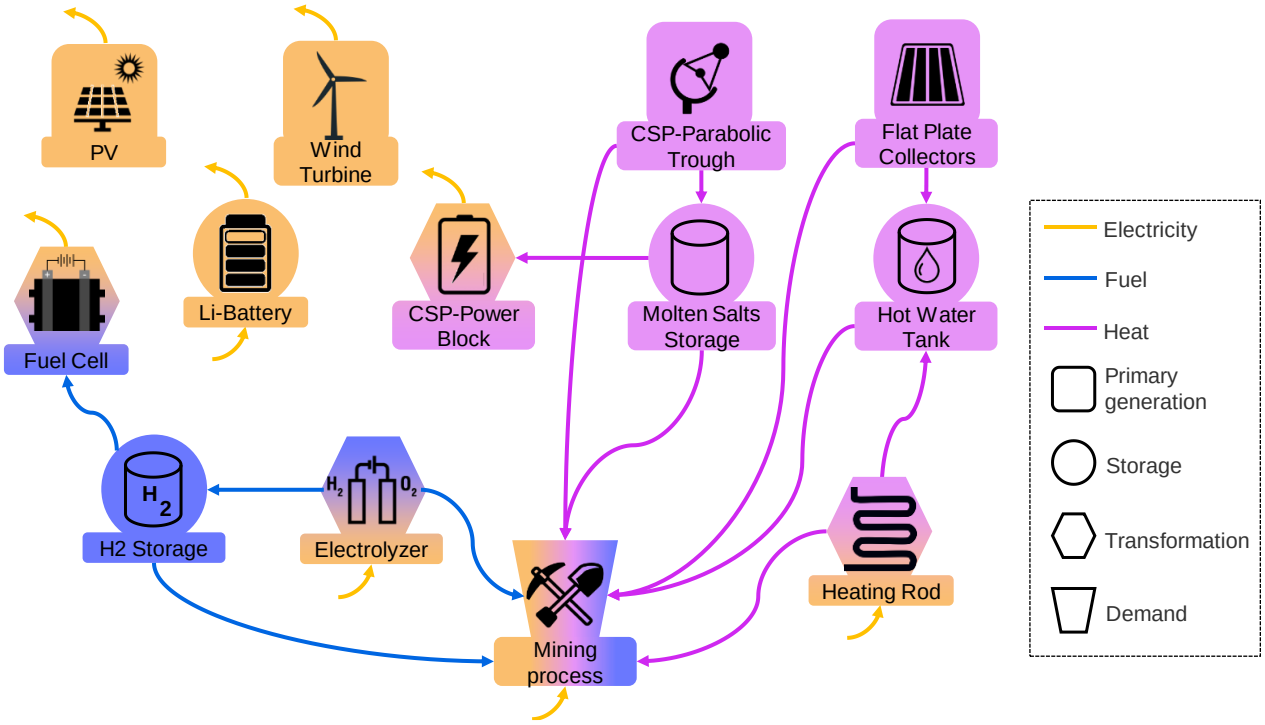

Fig. 5: System superstructure for the case study.

For this case study, we consider an earthquake as a disruption. An earthquake will affect the power that each technology might deliver. For example, for PV, this disruption may affect the connection to the grid or cause damage to a single panel, producing unserved energy to the process.

3. Chapter 3: Resilience Metrics

This section reviews the existing literature on resilience metrics. We revise 60 studies on resilience, then we select those that we considered that can be adapted to energy system planning and analyzed them in more detail. First, we show the field of application of the articles, then we offer more details on the selected ones on a table, and finally, we discuss some selected metrics to adapt one to our study.

3.1 Literature Review on Resilience Metrics

Resilience is applied to many engineering fields. Fig. 6 summarizes the area of application of the reviewed metrics. The most studied field is infrastructure and transportation, while resilience in power systems accounts for a minor share. Although there are some studies that use resilience metrics in power systems, a resilience indicator for multi-energy systems has not been observed. Accordingly, the indicator we introduce in the next sections aims at filling this gap.

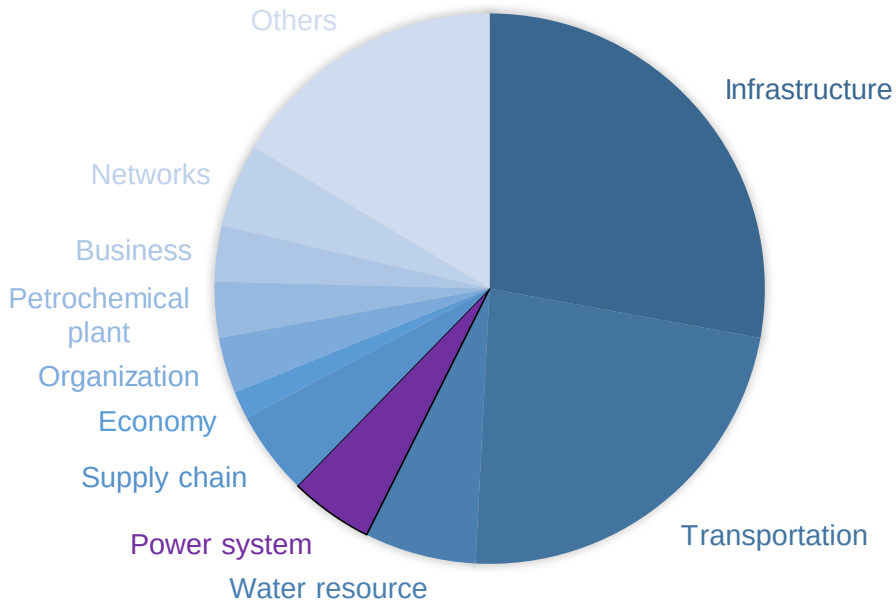

Fig. 6: Application area of the different metrics. 60 metrics analyzed.

From the revised studies on resilience, we select some metrics that we consider can be adapted to the field of MES. Selected metrics are summarized in Table 1. The metrics are described with some specific features: type of extreme event, application area, uncertainty considerations (deterministic or probabilistic), and time modeling (dynamic or stationary). In the following table, we summarize the selected studies.

Table 1: Some resilience metrics proposed in the literature.

Resilience Metric	**Recover from**	**Application field**	**Deterministic/ probabilistic**	**Stationary/ dynamic**	**Reference**
$R = \int_{t_0}^{t_1} [100 - Q(t)]dt$	Earthquakes	Community	Deterministic	Dynamic	[7]
$R = \int_{t_0}^{t_1} [100 - Q(t)]dt,$ $Q(t) = 100 - [L \cdot f_{rec} \cdot \alpha_R]$	Earthquakes	Infrastructure	Probabilistic	Dynamic	[15]
$R(X,T) = 1 - \frac{XT}{2T^*}$	-	-	Deterministic	Dynamic	[8]
$R(X,T) = 1 - \frac{XT}{2T^*} + \alpha\left(\frac{XT}{2T^*}\right)$	-	-	Deterministic	Dynamic	[16]
$R_j = \sum_i w_i \int_{t_0}^{t_1} [100 - q_i(t)]dt$	-	Energy	Deterministic	Dynamic	[17]
$R_L = \frac{dS(t)}{dt}, \qquad R_T = \int_{t_b}^{t_e} \frac{dS(t)}{dt}$	Human accident occurrences	Transportation	Deterministic	Dynamic	[18]
$R = E\left(\sum_w d_w / \sum_w D_w\right)$	Natural or human caused disaster	Transportation	Deterministic	Dynamic	[19]
$R = \frac{1}{P_d E_0} \int_0^{P_d} E(P_r) dP_r$	Earthquakes	Infrastructure	Probabilistic	Dynamic	[20]

$R = \frac{\%DDY^m - \%DDY}{\%DDY^m} = \frac{Y_D - Y_0}{Y_N - Y_0} = \frac{B}{A}$	-	Economic	Deterministic	Stationary	[21]
$R_{network} = \frac{V_{init} - V_{loss}}{V_{init}}$	Undersea earthquakes, fish bites or ship anchors	Internet networks	Deterministic	Stationary	[22]
$R = \frac{Recovery(t)}{Loss(t_d)} = \frac{F(t_r \mid e_j) - F(t_d \mid e_j)}{F(t_0) - F(t_d \mid e_j)}$	External disruptive event	Transportation	Deterministic	Stationary	[23]
$R_\varphi(t_r \mid e^j) = \frac{\varphi(t_r \mid e_j) - \varphi(t_d \mid e_j)}{\varphi(t_0) - \varphi(t_d \mid e_j)}$	-	Water resource	Probabilistic	Stationary	[24]
$R_\varphi(E, [0, T_C]) = \frac{\frac{1}{\lvert E \rvert}\sum_E \int_0^{T_C} \varphi(t; N, L, C)}{\int_0^{T_C} \varphi^{nominal}(t; N, L, C)}$	Terrorist attacks, natural disasters or manmade hazards	Infrastructure	Probabilistic	Dynamic	[25]

Bruneau et al. (2003) propose an indicator to measure the size of the expected degradation in quality (Q) over time due to an earthquake. This metric is deterministic and dynamic. Later, Bruneau and Reinhorn (2007) improved the same index with a more detailed measure of functionality. It considers the loss function (L), which is measured as the ratio of the actual loss, the recovery function (f_{rec}) after the time occurrence, which depends on the resources available during the recovery period, and the functionality recovery factor (α_R). The second term considers probability functions from fragility curves [26], being a probabilistic index.

Zobel (2010) proposed a simplification of the metric proposed by Bruneau et al. (2003). They calculated the loss function as a linear function and the total loss of functionality as the area of a triangle, in terms of the initial impact (X) and the recovery time (T). They also incorporated a time horizon (T^*), which allows to represent resilience as a percentage [8]. Later, Zobel (2011) adjusted this resilience function by giving different importance (α) to the initial impact of the disaster event and to the recovery time, by adding a new parameter to adjust the slope of the resilience function [16].

The metric proposed by Afgan and Veziroglu (2012) was also based on Bruneau et al. (2003) index. However, they developed a resilience index considering sustainability dimensions, which is a linear agglomeration function of products between indicators and the corresponding weighting coefficients (w_i) [17].

Enjalbert et al. (2011) defined the concept of *local resilience* (R_L) and *total resilience* (R_T), where the local resilience is an instantaneous measurement of resilience and is the slope of the resilience curve (S). It can be negative or positive if the performance decreases or increases, respectively. The total resilience is the sum of local resilience during a given period [18].

Chen and Miller-Hooks (2011) developed a similar indicator to that of Zobel (2010), measuring the fraction between the loss and total functionality. In this case, they define resilience as a fraction between the demand that can be satisfied after the event (d_w) and the pre-disaster satisfied demand (D_w) [19].

Franchin and Cavalieri (2015) described resilience in a new field: civil infrastructure. Their metric is a measure of the reallocated population ($E(P_r)$) due to an earthquake. They also considered uncertainty and vulnerability factors and how they affect resilience [20].

All the above-mentioned metrics consider the behavior of the system over time to measure resilience. There are other stationary indexes [21, 23, 24, 27], which measure the robustness of the system. These indexes are defined as a fraction between the system health after the event and before. They just differ in their application field.

3.2 Discussion of Some Metrics Related to this Study

From these metrics, we highlight the index proposed in [7], which measures the lack of system health over time. Graphically, this refers to the area over the resilience curve, as it shows in Fig. 7.

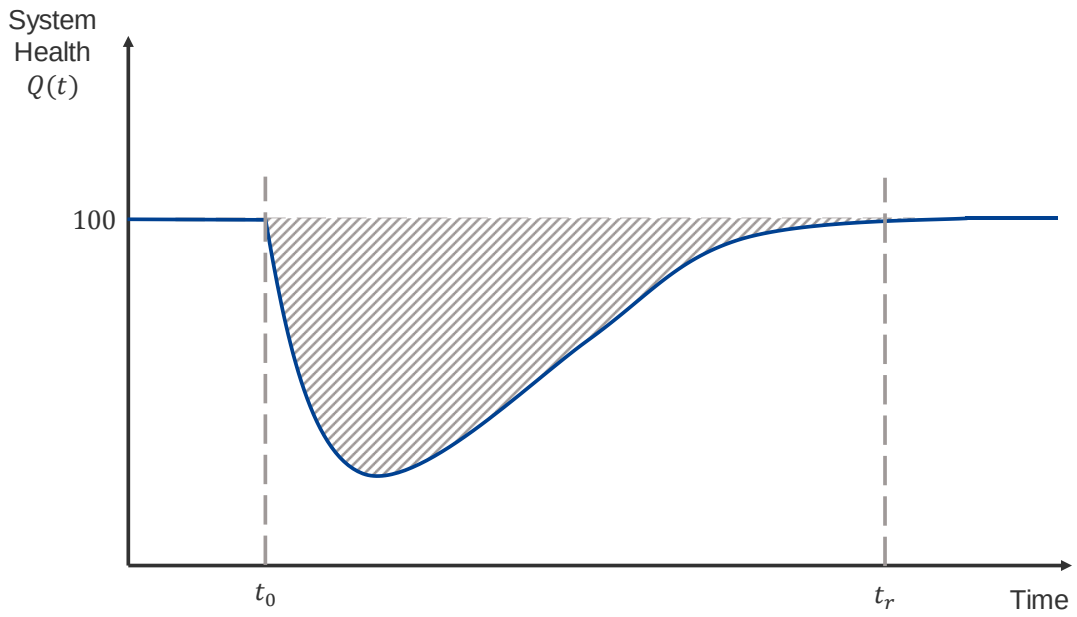

Fig. 7: Graphic representation of the metric proposed in [7].

This metric can be easily adapted to our study considering the lack of system health as the energy not supplied over time. This energy can be expressed as the difference between the energy demand during time $D(t)$ and the power that the system can deliver after a disruptive event $P(t)$. Mathematically:

$$R = \int_{t_0}^{t_r} [D(t) - P(t)]dt \qquad \text{(eq. 1)}$$

Or for a discrete case:

$$R = \sum_{t} [D(t) - P(t)] \qquad \text{(eq. 2)}$$

Graphically we can represent this equation as shown in Fig. 8.

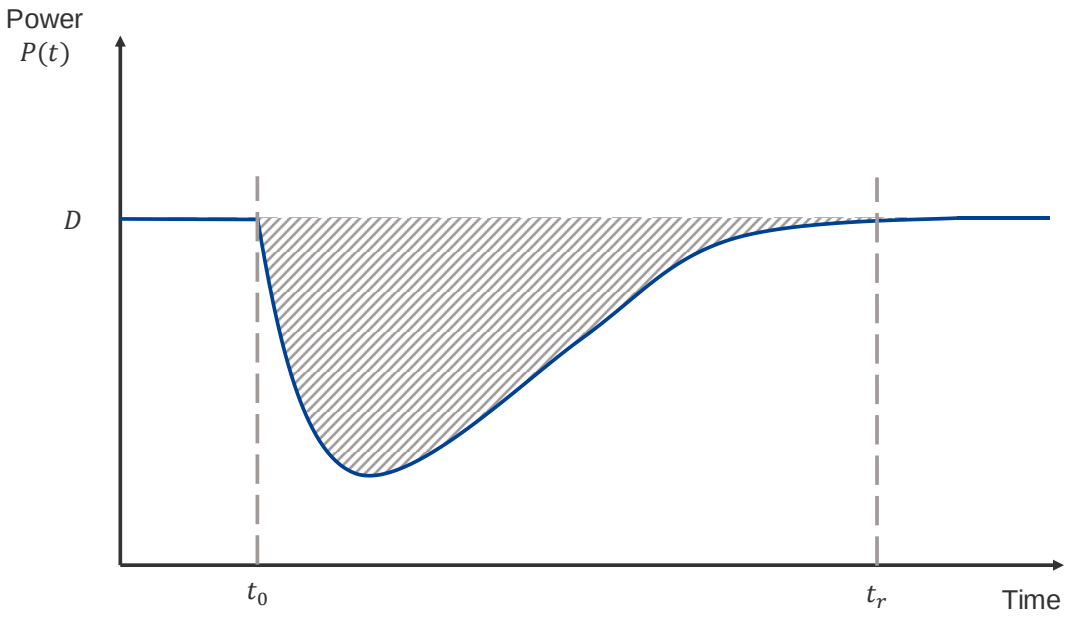

Fig. 8: Adaptation of the metric proposed in [7].

For this study we have a multi-vector energy system (different types of energy), therefore the total energy not supplied is the summation of each energy type:

$$R_T = \sum_i \sum_t [D_i(t) - P_i(t)] \qquad \text{(eq. 3)}$$

A

The problem with this metric is that it does not measure the resilience as we understand it. If the system's resilience increases, the value of the metric should increase, and the opposite happens with this metric, because if the system is resilient the energy not supplied should be less (smaller area). Therefore, we call the term "energy shortage" (ESh).

$$ESh_T = \sum_i \sum_t [D_i(t) - P_i(t)] \qquad \text{(eq. 4)}$$

Another problem with this metric is that the obtained value is difficult to compare in different case studies because the value is specific for each case (as total energy). Therefore, we expect a normalized metric.

Taking both problems into account, we consider the metric from [8], which defines resilience as the fraction between the post-event system health over time and the one in normal conditions. In this study they consider the reposition as a lineal function:

$$R(X,T) = 1 - \frac{XT}{2T^*} \qquad \text{(eq. 5)}$$

This is shown graphically in Fig. 9, where the resilience is the fraction between A_2 and the total area ($A_1 + A_2$).

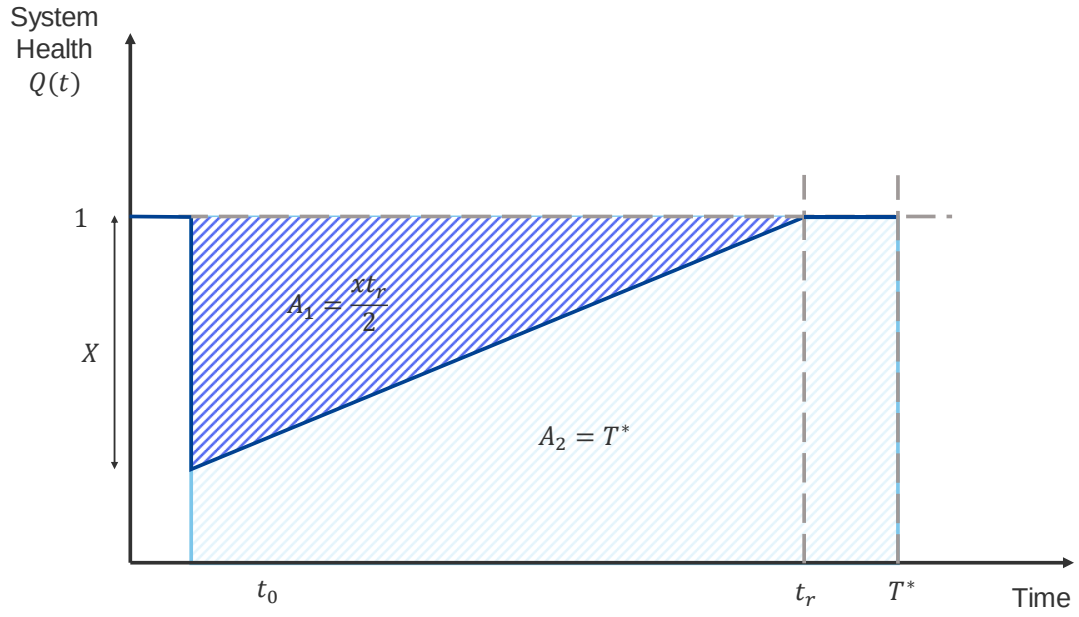

Fig. 9: Graphic representation of the metric proposed in [8].

The problem with this metric is that the recovery function can be non-linear. Therefore, we consider both metrics and use an adaptation of them. This new indicator is the fraction between the energy shortage of the system post-event and the total demand in a given time, as is shown in Fig. 10.

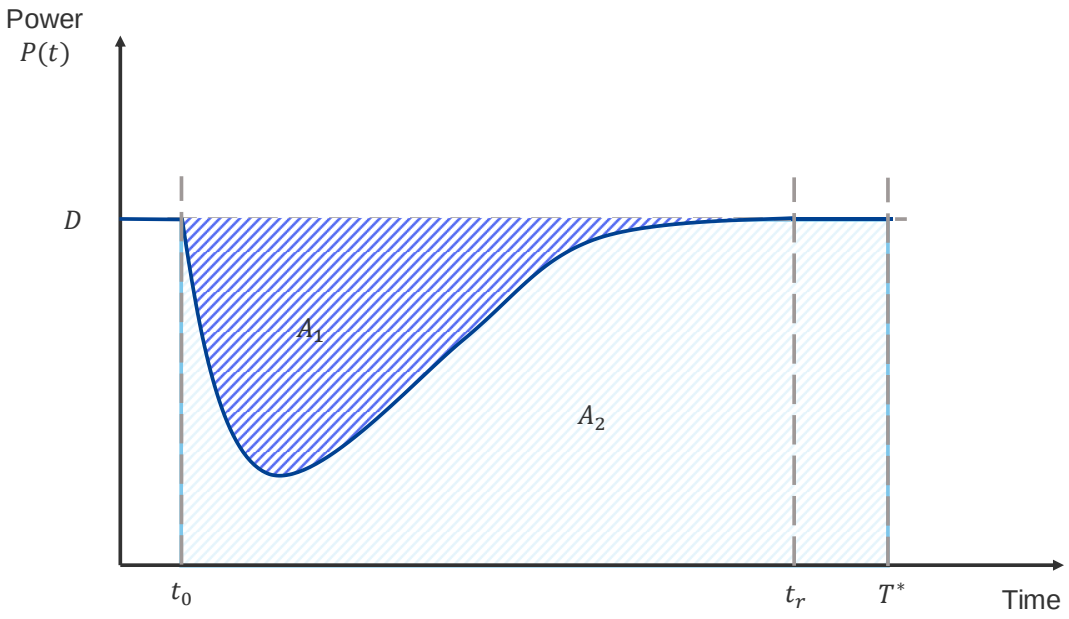

Fig. 10: Graphic representation of the proposed metric, considering [7] *and* [8].

From the graphic, we define the metric as:

$$R = \frac{A_2}{A_T} = 1 - \frac{A_1}{A_T} \qquad \text{(eq. 6)}$$

For this case, considering equation (eq. 1), this can be expressed as:

$$R = 1 - \int_{t_0}^{T^*} \frac{ESh(t)}{D(t)}\, dt \qquad \text{(eq. 7)}$$

Or for a discrete case:

$$R = 1 - \sum_{t_0}^{T^*} \frac{ESh(t)}{D(t)} \qquad \text{(eq. 8)}$$

As the metric should consider a multi-vector energy system, the total resilience is the summation of the weighting of all specific-energy resilience (R_i):

$$R_T = \frac{\sum_i R_i \cdot E_B^i}{D_T} \qquad \text{(eq. 9)}$$

In this section, we reviewed existing resilience metrics. The literature review shows a lack of resilience metrics for power systems and specifically, a resilience metric for multi-energy has not been observed. Therefore, we adapt a metric from the existing ones. This metric quantifies the energy shortage of the system. This is analog to the existing metrics but extended to multi-vector systems using weighting factors and considering models for the recovery of the components after an extreme event.

4. Chapter 4: Operational Simulation and Resilience Measurement

In this section, we simulate a disruptive event in an applied case. Given the resilience curve we measure the resilience using the metric previously described. First, we give the structure of the optimization problem. Then, we present the results of the simulation in an applied case. The work presented in this section is important to develop a new indicator because the results are used as a reference in the next section.

The case study is the same from section 2.4, which is already planned by [14] considering only an economic indicator. The value of the installed capacity of each technology is used as input in this section and the values are detailed in appendix D.

4.1 Structure of the Operational Simulation

For an operational simulation of a system dealing with a disrupting event is necessary to know the reposition curves of each technology, which are detailed in Appendix E. With these parameters, the behavior of each technology given an event is known and it is possible to perform an operational simulation to obtain the optimal configuration of the system over time. The optimal configuration is obtained minimizing the not supplied energy. Therefore, we minimize the energy shortage described in (eq. 4):

$$\min ESh_T = \sum_i \sum_t [D_i(t) - P_i(t)] \qquad \text{(eq. 10)}$$

This energy shortage is described as an energy balance, considering the power demand and supply of each technology for each process over time ($P_{b,tec}(t)$).

This power could change after an event, cause the maximum available capacity could be affected by the damage caused. This damage is given by the restoration curve ($RC(t)$), which is considered a fraction of the original capacity, depending on time. Therefore, the maximum capacity is given by the following equation:

$$P_{b,tec}^{av}(t) = \begin{cases} P_{b,tec}^{inst}, & t < t_0 \\ P_{b,tec}^{inst} \cdot RC(t), & t_0 \leq T \end{cases} \qquad \text{(eq. 11)}$$

This can be graphically described in Fig. 11:

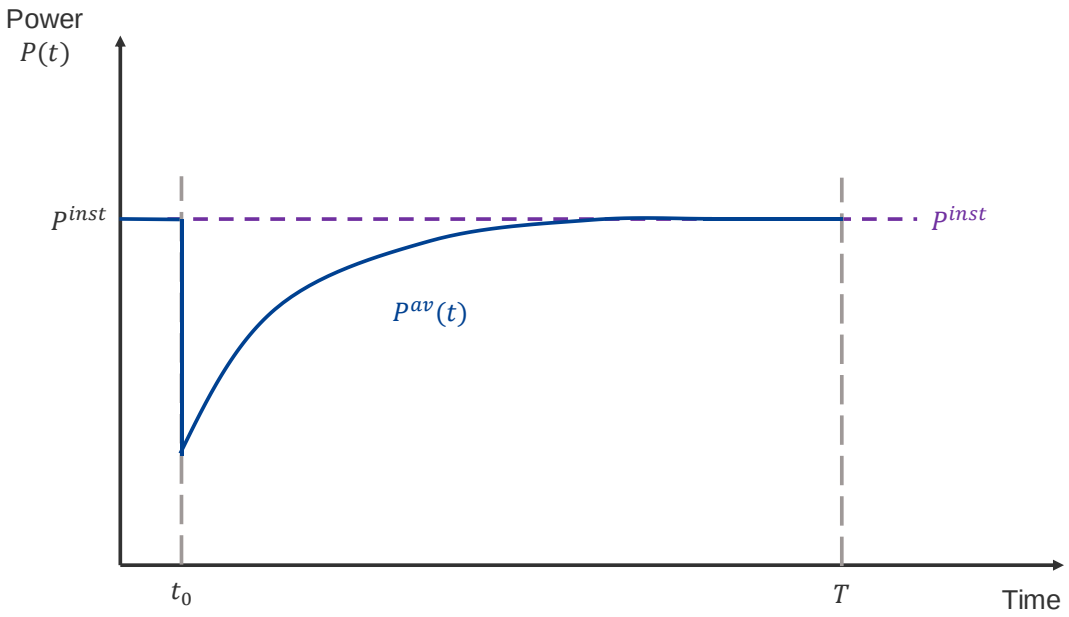

Fig. 11: Graphical representation of the power capacity installed over time given a disruptive event.

This maximum power capacity is introduced to the optimization problem as a constraint, where the power delivered should be less or equal than the available capacity:

$$P(t) \leq P^{av}_{b,tec}(t) \qquad \text{(eq. 12)}$$

4.2 Results in Applied Case

After the problem is optimized, we can measure the resilience as it was described in the previous section, with (eq. 9).

To study this metric, we use the case study described in Section 2.4. The installed capacity and restoration curve of each technology are presented in Appendix D and E, respectively. For this study, we used a time horizon of one year, a PGA (Peak ground acceleration) of 0.6g, which is similar to an earthquake of $8M_{ww}$, and the time when the event occurs is the first hour of the year (01:00 January 1st).

The resulting resilience is 80%. This means that for a PGA of 0.6, this system can provide 80% of the total energy demand in one year. This is equivalent to two and a half months of a blackout, which is a long period of time.

The resilience value is an arbitrary value, which depends on the time horizon and the PGA of the earthquake.

On the other hand, the simulation provides us information about the expected served energy over time, which is shown in Fig. 12. The served energy is normalized by the total demand.

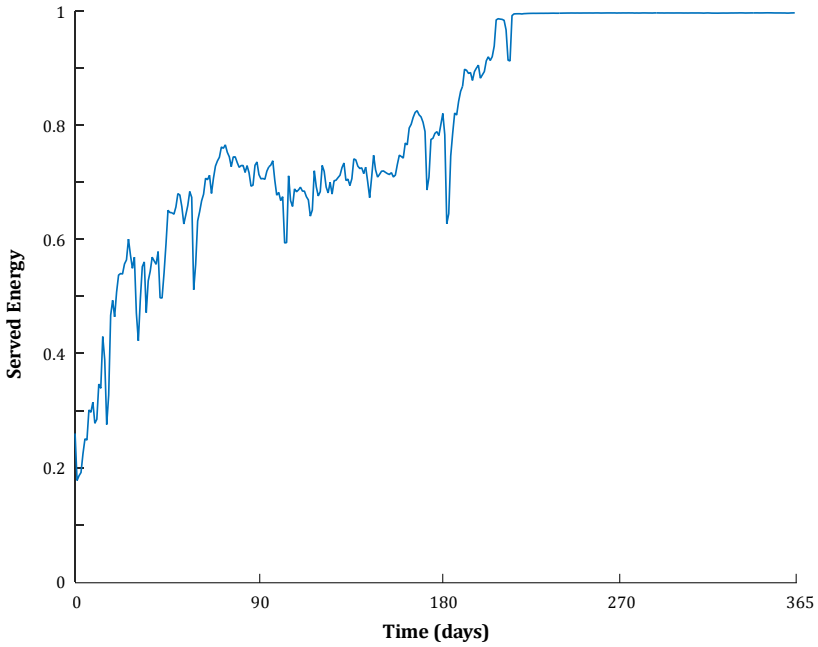

Fig. 12: Served energy of the system over time. Values are normalized by the total demand.

The peaks of the curve are explained by the energy demand of the systems, which is not linear. From the figure, we can see that the system is completely recovered in 220 days, which is a long-time period.

This is consisting with the expected result, according to the shape of the curve, which grows gradually as the restoration of each technology. However, is difficult to compare to reality, because there is no existing autonomous MES affected by an earthquake.

A limitation of this metric is that the value of this indicator depends directly on the time horizon, which is an arbitrary selection. For this study, we used a time horizon of one year, but this may change depending on the study. Increasing the time horizon should increase resilience because we are considering the time where the system already recovered, so the fraction between the shortage and the total demand will decrease. The opposite should happen by decreasing the time horizon. Despite the arbitrariness, as it is a percentage, it is easy to compare the resilience of different system configurations. However, to compare the resilience of different scenarios, the time horizon should be the same.

The system depends fully on renewable energy and most of the solar energy as the primary generation, so it is important to consider the weather. In the present analysis, the time of the earthquake t_0 was fixed in the first hour of the year (00:00, January 1st). Since

the case study is in Chile (southern hemisphere), that is in the summertime. Then, the availability of solar energy is higher than at other times of the year. To compensate for the reduced capacity factor in winter, the system has more installed capacity of PV than it requires in summer. This would lessen the impact of losing generation capacity during summer. In other words, it should be harder for the system to compensate for the damage in solar generation during winter than during summer. However, the event may occur at any time during the day and any day of the year, so if the event occurs in winter, we expect a lower value of resilience. Therefore, the resilience of the system may also depend on the time of the event.

In this section, we performed an operational simulation and we measured the resulting resilience given a disrupting even. To simulate the system operation after an event we used the adapt metric in an LP problem. We used restoration curves as input. The objective function was to minimize the energy shortage of the system. While the main constraint is that the power delivered for each technology cannot exceed its restoration curves. This was possible to apply to our case study and the results are consisting of the expected.

5. Chapter 5: A New Resilience Indicator for the System Design

In this section, based on the literature review and the methodology of the previous section, we propose a new indicator to plan with resilience of a multi-energy system. We expect to use this indicator in planning decisions as an OF in a MOP.

The methodology of this section is an iterative process, where we use the value obtained from the previous section as a reference for the development of the new indicator. However, only the final result is presented.

The proposed indicator considers the possible energy shortage in the system due to an earthquake. This indicator requires as inputs the performance of the energy technologies (energy demand and supply of each technology over time, considering efficiency and generation profile for variable renewable energy), the energy demand, and the technologies behavior in the case of facing an earthquake (described by the restoration curve).

The indicator we propose describes the resilience of the system as a percentage that shows the energy that the system can supply after a disruptive event about the total energy demand in an evaluation horizon. To determine the energy that the system can supply, we need to measure the non-supplied energy (energy shortage) of each energy vector to obtain the total shortage. This is analog to the loss of energy expectation (LOEE) in power systems but extended to multi-vector systems using weighting factors and considering models for the recovery of the components after an extreme event. We evaluate the damage of each component of the system and count the energy demand that cannot be satisfied as a result of this damage. This is done for each vector and the total resilience is a weighted sum.

5.1 Maximum Power Available

As this indicator quantifies the possible energy shortage to the process, we need to know the behavior of each technology during the time, represented in their power capacity. This is illustrated in Fig. 11, where the maximum power available is described by $P^{av}(t)$. This power can be mathematically described as follows:

$$P_{b,tec}^{av}(t) = \begin{cases} P_{b,tec}^{inst}, & t < t_0 \\ P_{b,tec}^{inst} \cdot RC(t), & t_0 \leq t \end{cases} \quad \text{(eq. 13)}$$

Where P^{inst} is the power of the technology previously installed, $RC(t)$ is the restoration curve, t_0 is the time of the day where the event occurs, t_{rec} the expected recovery time, and T^* the time horizon of the evaluation.

The energy delivered or consumed by each technology changes over time. Fig. 13 a) shows a possible power delivered by a technology $P(t)$. The real power delivered by this technology $P_r(t)$ after an event is the minimum between both functions as is shown in Fig. 13 b).

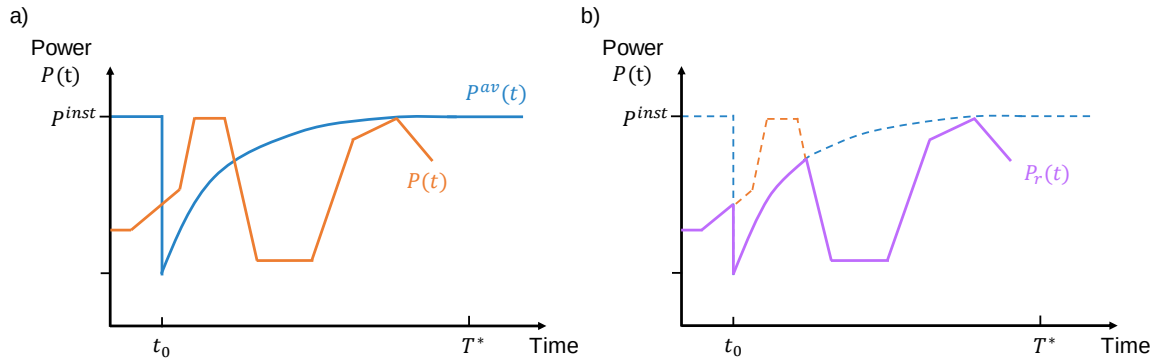

Fig. 13: Power delivered or consumed by each technology due to an event.

Mathematically we will express that as follows:

$$P_r(t) = \min\{P^{av}(t), P(t)\} \qquad \text{(eq. 14)}$$

Or in a linear optimization model

$$P_r(t) \leq P^{av}(t)$$
$$P_r(t) \leq P(t) \qquad \text{(eq. 15)}$$

We do the same procedure for each technology.

5.2 Energy Shortage Measurement

To define the resilience of the system we need to measure the non-supplied energy. Therefore, we measure the energy shortage (Sh) in every time for each energy type i $\left(ShP_i(t)\right)$, through an energy balance. This balance is the difference between the demand and the supply of that energy type. The power demand is the summation of the demand of the process P_D^i, the demand for the transformation technologies $P_{TT}^{i,j}$, (demand i to

produce j), and the power required by the storage load $P_S^{load,i}$. The supply corresponds to the power produced from the primary generation P_{PG}^i, the supply from the transformation technologies $P_{TT}^{j,i}$, and the power given by the storage unload $P_S^{load,i}$. This can be summarized in the following equation:

$$ShP_i(t) = \left(P_D^i + \sum_j P_{TT}^{i,j} + P_S^{load,i} \right) - \left(P_{PG}^i + \sum_j P_{TT}^{j,i} + P_S^{unload,i} \right) \quad \forall i, j \epsilon I \quad \text{(eq. 16)}$$

If this difference is positive, there is an energy shortage; if it is negative, the system can supply the demand. In consequences, the shortage is the maximum between this difference and zero:

$$ShP_i^+(t) = \max\left(0, ShP_i(t)\right) \qquad \forall i, j \epsilon I \qquad \text{(eq. 17)}$$

Or in a linear optimization model

$$\begin{gathered} ShP_i^+(t) \geq 0 \\ ShP_i^+(t) \geq ShP_i(t) \end{gathered} \qquad \forall i \epsilon I \qquad \text{(eq. 18)}$$

The total energy shortage is its integration over time:

$$Sh_i = \int_{t_0}^{T^*} ShP_i^+(t)\,\mathrm{dt} \qquad \forall i \epsilon I \qquad \text{(eq. 19)}$$

5.3 Resilience Measurement

With this shortage, we can calculate the resilience for this energy vector as one minus the fraction between the energy shortage and the demand of that vector $\left(E_D^i\right)$:

$$R_i = 1 - \frac{Sh_i}{E_D^i} \qquad \forall i \epsilon I \qquad \text{(eq. 20)}$$

As it is a multi-vector energy system, the total resilience is the summation of the weighting of all individual resilience values:

$$R_T = \sum_i \left(R_i \cdot \frac{E_D^i}{\sum_j E_D^j} \right) = \frac{\sum_i E_D^i - \sum_i Sh_i}{\sum_i E_D^i} \qquad \text{(eq. 21)}$$

This indicator, in contrast to other resilience metrics, can be easily integrated into the planning process. This is because of the linear nature of the index. Using LP is a common practice in energy systems planning. This allows for computational tractability in large scale problems. Our index also allows keeping the optimization linear. It can be included as an optimization function.

A limitation of this indicator is that it does not consider the re-design of the system to deliver energy after the event. This is analyzed in Chapter 6, where the resilience value of the indicator is compared to the value obtained through an operational simulation of the system after the event.

Another limitation of the indicator is the time of occurrence of the event. The result of the resilience value may change depending on the time of the event. Therefore, we can analyze this problem changing many times this variable and analyzing the results.

This section presents the development of a new resilience indicator to design a MES. It measures the energy shortage of the system in case of a disrupting event. It uses weighting factors for the different energy vectors and considers models for the recovery of the components after the event. This indicator can be integrated into planning decisions, because of its linear nature.

6. Chapter 6: Planning a Resilient and Low-cost Multi-energy System

In this chapter we proved the methodology of the proposed framework described in Chapter 2, dividing this chapter into 3 sections, accordingly to the methodology stages:

1. Investment planning: we use the previously created resilience indicator and an economic indicator (costs) to plan a MES. With this purpose, we solve a MOP with different weights to study the trade-off between both objective functions and analyze 3 scenarios.
2. Operational simulation: we follow the same methodology as Chapter 4. We use as input the installed capacities of the chosen scenarios, obtained by the previous section. We simulate a disruptive event using restoration curves, and we measure the resulting resilience.
3. Resilience index validation: To validate the index, we perform an operational simulation with the MCM and we compared it with the result obtained using restoration curves.

6.1 Investment Planning

For investment planning, we need to solve a MOP with two objectives functions: resilience and costs. Therefore, we use a normalized constraint method, where the objective function is the costs of the system, while the resilience is modeled as a constraint varying the weight of the target.

$$\min_{x \in R^n} f(x) = f_{ec}(x)$$

$$subject\ to \quad c_{re}(x) = \frac{f_{re}^{bc}(x) - f_{re}(x)}{f_{re}^{bc}(x) - f_{re}^{wc}(x)} \leq \omega_{re} \qquad \text{(eq. 22)}$$

$$= f_{re}(x) \geq \omega_{re} \cdot \left(f_{re}^{bc}(x) - f_{re}^{wc}(x)\right) + f_{re}^{bc}(x)$$

To use this method, we need to know the best and the worst case for the objective function to be modeled as a constraint. For resilience, the best case is the maximum value, which was set in 99% and the worst case is the minimum, which is achieved when the cost is minimum. Table 2 presents the maximum and minimum value for both objective functions.

Table 2: Value for the worst and best case of each objective function.

Target	f^{wc}	f^{bc}
Costs $(€/MWh)$	53.6	26.4
Resilience $(-)$	0.80	0.99

With those values, we solve the MOP for different weights of resilience to obtain a Pareto front, presented in Fig. 14.

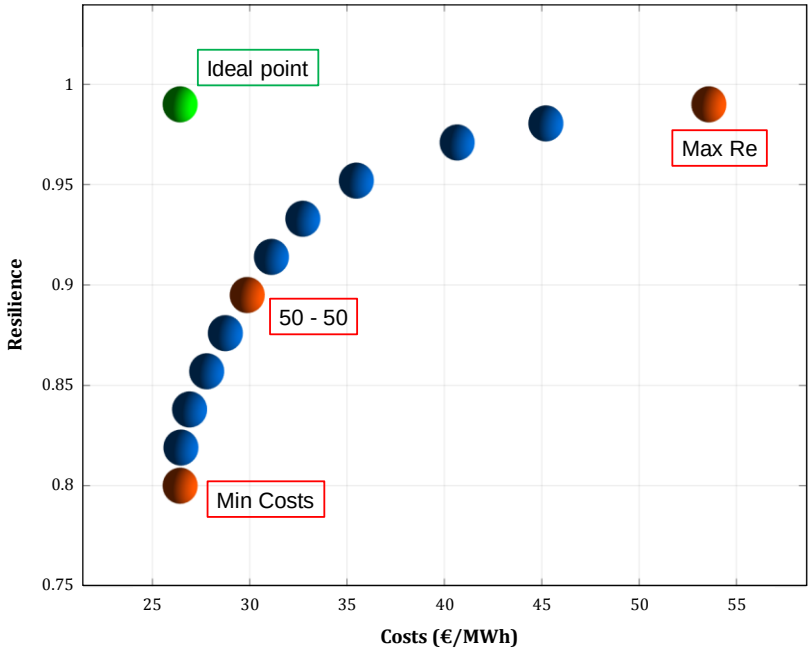

Fig. 14: Pareto front between resilience (y-axis) and costs (x-axis).

From the Pareto front, we can note a trade-off between the resilience and the cost: increasing the resilience means a higher cost for the system. Specifically, to increase resilience by 20% (from the lowest to the highest value) it is necessary to double the installation cost.

On the other hand, we can see that in high values of resilience, increasing this target is more expensive than in lower values. For example, increasing the resilience from 97% to 99% implies an installation cost 32% higher, and increasing this value from 80% to 82%, implies increasing the installation cost just by 0.2%.

To study the effect of including resilience on planning decisions, we analyze three cases pointed with red in Fig. 14: (1) minimum cost, (2) weight of 50% of resilience and (3) maximum resilience. The results for costs and resilience for these cases are detailed in Table 3. Appendix F shows detailed results.

Table 3: the value of resilience and costs for 3 scenarios.

	$\boldsymbol{min\ Cost}$	$\boldsymbol{50-50}$	$\boldsymbol{max\ Re}$
$\textbf{Costs}\,(€/\boldsymbol{MWh})$	26.4	29.9	53.6
$\textbf{Resilience}\,(-)$	0.80	0.90	0.99

For these three scenarios, we analyze the predicted served energy over time, as shown in Fig. 15. From the figure we can see that increasing the value of the resilience, the total served energy increases, as is expected.

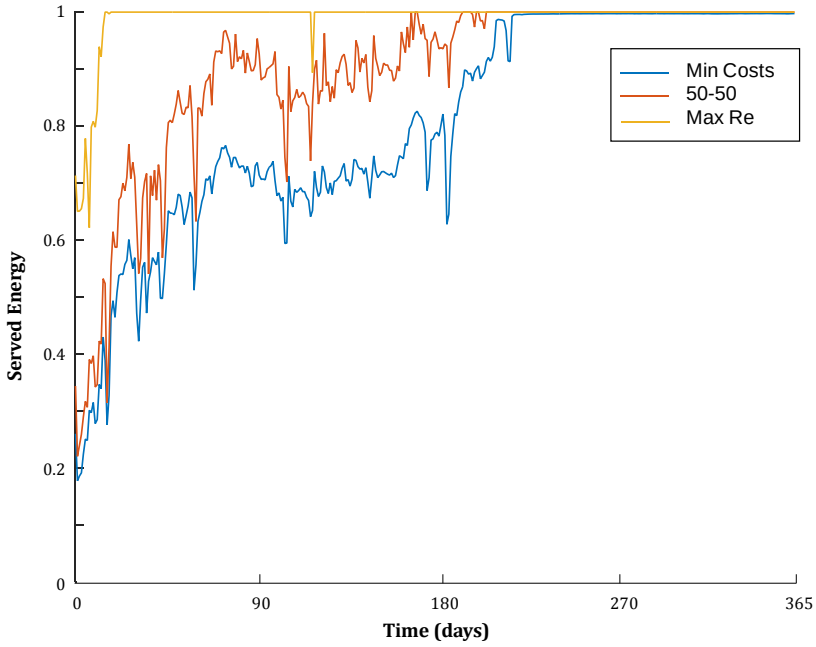

Fig. 15: Served energy over time. The values of energy are normalized by the total demand.

6.2 Operational Simulation

For these three scenarios, we perform an operational simulation. We follow the same methodology described in Chapter 4, where the goal is to minimize the energy shortage. Like in the planning stage, we use restoration curves. However, in this stage, we use as input the installed capacities obtained from the previous stage and we simulate the system operation after the event.

The operational simulation gives the system the freedom to adapt its operation minimizing the energy shortage. This differs from the planning stage, where the power delivered after the event is constraint by the scheduled power, defined by (eq. 15). Therefore, we expect that the resilience value obtained for the operational simulation using restoration curves is equal or better the expected in the planning stage.

The results are shown in Table 4 and Fig. 16. Table 4 shows the predicted values from the indicator in the first row, previously described, and the second row shows the operational simulation. Fig. 16 shows the served energy, comparing the predicted result using the indicator and for the operational simulation for the different scenarios.

Table 4: The value of resilience for 3 scenarios. The first row shows the predicted values from the indicator, the second row the resulting value through an operational simulation using restoration curves (RC).

	$min\ Cost$	$50-50$	$max\ Re$
Indicator	0.80	0.90	0.99
RC	0.84	0.92	0.99
Difference	5%	2%	0%

From the table, we can see that the values of resilience for the indicator are underestimated compared to the obtained in the operational simulation. On the other hand, from Fig. 16, we can also observe this difference over time.

This difference is explained because of the difference in both models. For the indicator, the resilience is calculated from the energy that is supplied in normal conditions constraining the maximum power available for each technology. On the other hand, for the operational simulation the target is to minimize the unserved energy, given the model freedom to adapt the delivered power given the event.

However, the highest difference is 5% in the scenario of minimum costs, which makes this indicator a good approach for the resilience final value.

In this case, the operational simulation is modeled, as the indicator, with the restoration curves. The restoration curve is a smooth function and, in this context, means that the restoration of each technology will increase hourly, as is shown in Fig. 17 a). This may not be entirely correct. Therefore, we use another method to validate our index.

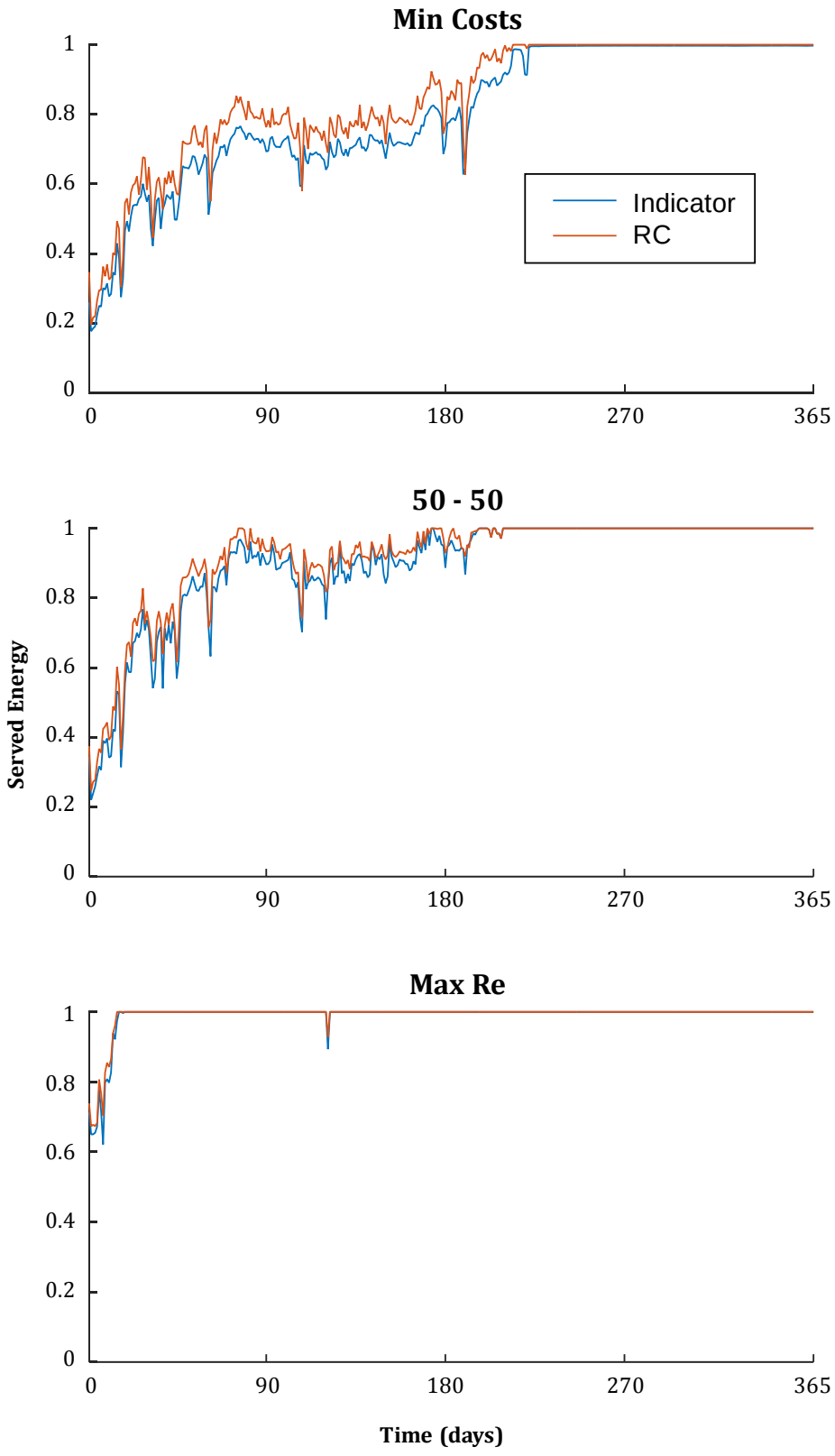

Fig. 16: Served energy for 3 scenarios. Comparison between the indicator and the case of operational simulation using restoration curves (RC). Value for energy is normalized by demand.

6.3 Resilience Index Validation

In real life, the restoration of the system includes uncertainty on the damage suffered and the restoration of each technology. Usually, the restoration of technology is defined as a one-step function, where is completely inactive and in a specific time is completely operative, as is shown in Fig. 17 b), and this restoration time is random.

In some cases, the system may have more than one technology of the same type and they might have different restoration time (e.g. PV) because different problems or not all of them will be completely inactive due to an earthquake. In this case, the restoration curve will be similar to the presented in Fig. 17 c), where the curve is a step function, and each step is the restoration of one technology.

In this case, if recovery time has the same distribution of the restoration curve given from fragility curves, as more technologies we have, the curve will be more like the curve presented in Fig. 17 a).

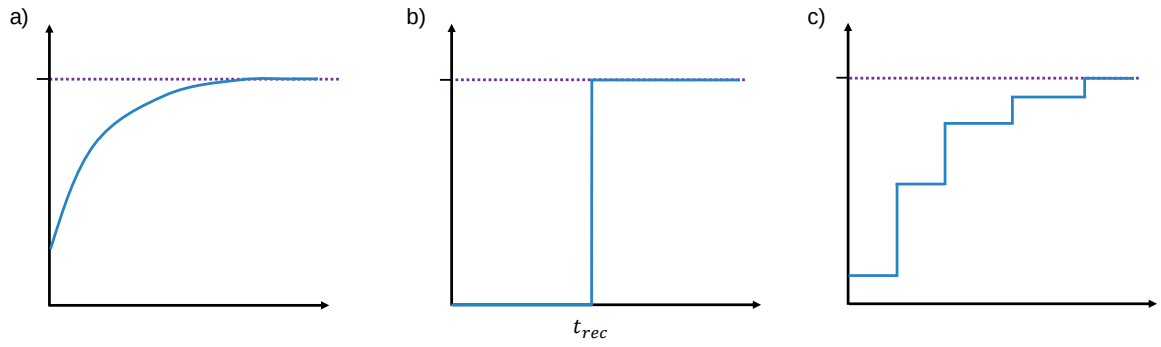

Fig. 17: Different scenarios for the restoration of the technologies. (a) represent the restoration curve used in planning decisions, (b) the step function used in the Monte Carlo simulation with random recovery time, and (c) is a graphic representation when you have more technologies of the same type.

To simplify the study, we consider that every technology restores as a one-step function, where the restoration time is a random variable, which its distribution is given from fragility curves. This means that the average of those values is the restoration curve. Therefore, we performed a Monte Carlo simulation (MCS).

As the average of these restoration times is the restoration curve, which is the same used in the previous operational simulation, we expect that the average value of the resilience in this validation through MCS will be similar to the obtained in the operational simulation with restoration curves.

We performed an MCS for the same three scenarios and simulated 500 cases for different restoration times. The mean resilience value for each scenario is shown in Table 5.

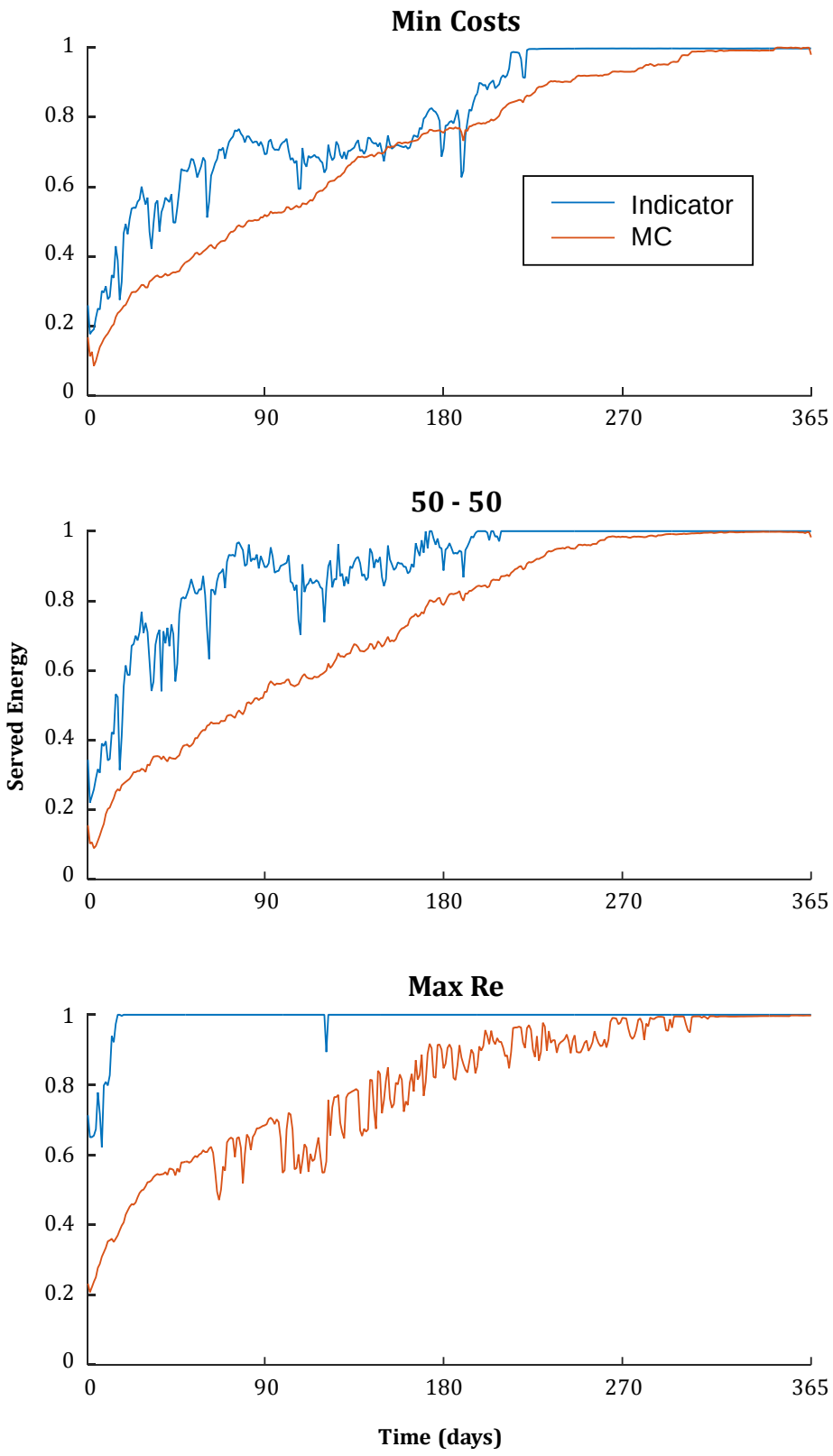

Fig. 18: Served energy for 3 scenarios. Comparison between the indicator and the case of operational simulation using Monte Carlo simulation (MC). Value for energy is normalized by demand.

Table 5: Resilience average value for 3 scenarios through operational simulation using restoration curves (RC) and through the Monte Carlo simulation (MCS), with the percentual difference.

	$min\ Cost$	$50-50$	$max\ Re$
Indicator	0.80	0.90	0.99
MCS	0.69	0.71	0.80
Difference	14%	21%	19%

From Table 5 we can see that the average value of resilience of the MCS is lower than the expected from the indicator, where the difference is around 20%. However, the tendency is similar, as increasing the expected resilience value, the average value of resilience increases. We can also observe this difference in Fig. 18, which shows the served energy for the three scenarios as the average value for each time for the 500 cases.

This behavior is also presented in Fig. 19, where it is shown the served energy of the three scenarios. The served energy of the scenario of maximum resilience is significantly higher than the other scenarios, while the curve for the scenario of minimum cost and 50%-50% are similar, which agree with the values from the table with a difference of 2%.

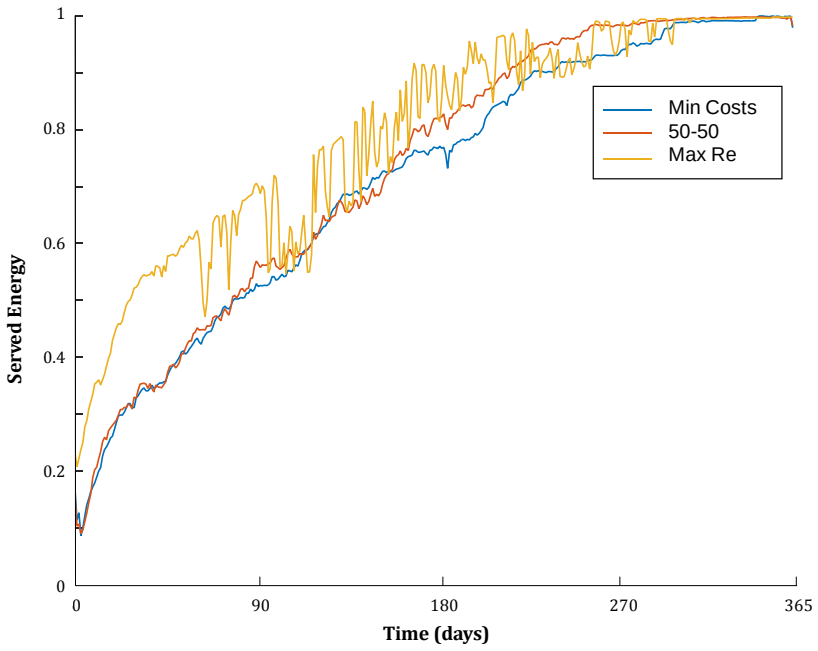

Fig. 19: Energy unserved over time. Monte Carlo Simulation.

The histogram of the Monte Carlo simulation for the three scenarios is shown in Fig. 20. We can see that the distribution is center in specific ranges, defined as the mode. These ranges are presented in Table 6.

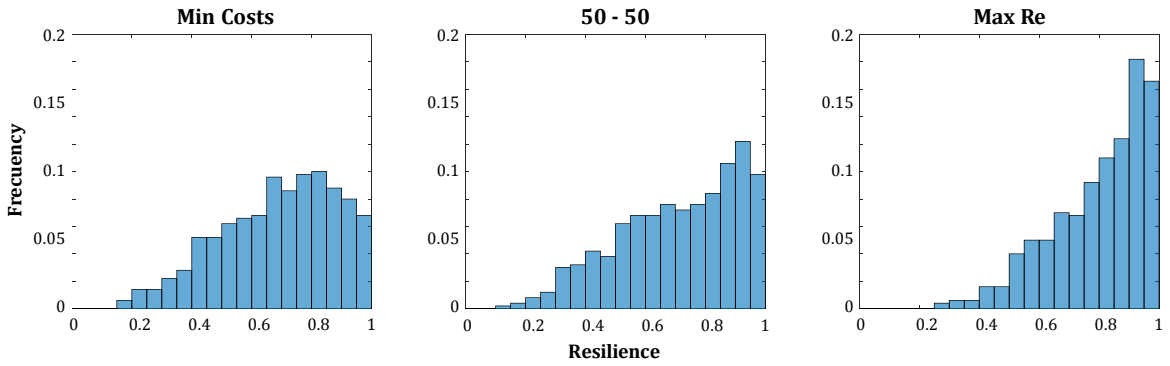

Fig. 20: Histogram for the resilience value through the Monte Carlo simulation. Values are normalized.

Table 6: Mode of the data of resilience through the Monte Carlo simulation for 3 scenarios.

	$\boldsymbol{min\ Cost}$	$\boldsymbol{50-50}$	$\boldsymbol{max\ Re}$
Mode	$[0.75-0.8]$	$[0.9-0.95]$	$[0.9-0.95]$

These values match better with the expected values, where the only value of the expected resilience out of the range is for the scenario of maximum resilience, in which the expected value is overestimated according to the MCS results.

The difference between the mode and the average value is related to the definition of resilience, which does not allow values greater than 1. This is given by the (eq. 17), where all the negative values of the energy shortage are set in zero.

Therefore, the expected value for resilience given by the indicator seems to be the value of the maximum probability of occurrence and not the average.

On the other hand, we can explain this difference by the different restoration curves used in this simulation and in the planning stages. The system integrates the different energy vectors. Therefore, the supply of each energy vector is subject to the performance of every technology. Therefore, the supply is directly subjected to the technology that restores the last, creating a "bottleneck" effect in the process.

In the case of the operational simulation using restoration curves, as every technology restores gradually, this bottleneck effect is not present, contrary to the MCS, where the technology with the highest value of restoration time creates the effect.

However, we think that we are underestimating this value, because, as we previously explained with Fig. 17, there are some technologies that can gradually recover, or the health of the technology might not be zero. For example, PV: if the process has many panels, they might have different restoration times, because of different problems, or not all of them will be completely inactive due to an earthquake, as shown in Fig. 17 c).

A limitation of this model is that it can be applied just for a process, where the location of each technology is not far away from each other. If that is the case, the transmission would have an important impact on the system, which is not considered in this model. On the other hand, this system considers a given PGA and it is the same for each technology, if they were in a larger distance the earthquake will affect them on different magnitudes, therefore, the PGA may change between technologies.

In conclusion, the resilience index is not completely validated, because MCS results of the resilience average differ in around 20% of the expected resilience value. However, integrate the resilience index has a positive effect on resilience because if we increase the weight of the resilience indicator, the system is more resilient.

This section is the final chapter, where we proved the methodology of the proposed framework. It was divided into three sections. The first section presents the investment planning of the system. We observed a clear trade-off between both OF through a Pareto curve. Improve the resilience of the system involves increasing costs. In the second section, we simulate the operation given a disruption. We saw that the recovery of the system was similar to the expected in the previous section. Specifically, it had a better recovery because it gives the model the freedom to adapt the delivered power given the event. The last section is a validation of the model using another method. We used step-functions instead of restoration curves. Therefore, we used an MCM, where the recovery time was the random variable. The average of the method shows that the resilience value was lower than the expected. This was explained because, as it is a coupled system, the step functions for the technology generates a “bottleneck effect”, where the technology with the highest value of restoration time affects the most the energy supply.

7. Conclusions

For this study, we developed a method to plan a multi-energy system (MES) optimizing its resilience and costs. This method had three stages: i) investment planning of a MES with two targets: resilience and costs, ii) operational simulation of the system in the case of a disrupting event, and iii) the index validation where we considered the restoration time uncertainty through a Monte Carlo simulation. To apply this method, this thesis has been divided into four chapters: a review of resilience metrics and the adaptation of a metric for our study, an operational simulation and measurement of resilience for a better comprehension of a new indicator creation; the creation of a resilience indicator for the system design, and the planning of a resilient and low-cost MES, in which all three method stages were applied.

The review of resilience metrics showed that most of the metrics are focused on measuring the lack of system's health, which is analog to the energy shortage of our study. Furthermore, we observed that resilience in power systems are barely studied. Specifically, a resilience indicator for multi-energy systems has not been observed. Accordingly, this work aims at filling this gap, adapting a metric for MES based on the review.

This metric was used to simulate the system operation in the case of a disrupting event. The simulation was a linear programming problem based on minimizing the energy shortage of the system in the case of an event.

Based on the operational simulation, we integrated this metric into planning decisions, creating a new indicator. This indicator describes the resilience of the system as a percentage to show the energy that the system can supply after a disruptive event in relation to the total energy demand in an evaluation horizon. In contrast to other resilience metrics, this indicator can be easily integrated into the planning process due to the linear nature of the index.

Finally, we planned a resilient and low-cost MES, using the proposed method. The results showed a clear trade-off between both targets, where increasing resilience involved an increase in costs. The operational simulation of the system after an event shows a higher value of resilience than predicted by the indicator since the model is free to adapt the power delivered, minimizing the unserved energy. To validate the model, we performed a Monte Carlo simulation. It showed lower values than expected, explained by the difference between the restoration curves used in the planning stage and in Monte Carlo simulation. Even though the values are lower than predicted, the increase in resilience is the expected; therefore, the method looks promising to plan a multi-energy system considering resilience in its design.

The model limitations are, on one hand, that the resilience indicator considers losses or degradation of the technologies, but not of the energy transmission since it was developed for a process and the distances between technologies are not considered. On the other hand, this system considers a given PGA, which is the same for each technology, if they were further away, the PGA may change between technologies. As a consequence, this is a forward-looking work that aims at adapting the present model to cover those limitations. We propose to adapt the indicator to consider the transmission of the system and its possible damage in the case of an earthquake and expand the case study to a region or even a country.

Glossary

CSP	Concentrated solar power
GW	Giga Watts
FEMA	Federal Emergency Management Agency
IPCC	Intergovernmental Panel on Climate Change
LP	Linear programming
MCM	Monte Carlo Method
MES	Multi-energy system
MOP	Multi-objective problem
PV	Photovoltaics
PGA	Peak ground acceleration
SOP	Single-objective problem

Bibliography

[1] SAWIN, J., RUTOVITZ, J. y SVERRISSON, F. 2018. Renewables 2018-global status report. 41 p.

[2] BROWN, T., SCHLACHTBERGER, D., KIES, A., SCHRAMM, S. y GREINER, M. 2018. Synergies of sector coupling and transmission reinforcement in a cost-optimised, highly renewable European energy system. Energy. 160: 720–739.

[3] MANCARELLA, P. 2014. MES (multi-energy systems): An overview of concepts and evaluation models. Energy. 65: 1–17.

[4] FEMA. Hazus –MH 2.1. 2015.

[5] HOSSEINI, S., BARKER, K. y RAMIREZ-MARQUEZ, J. 2016. A review of definitions and measures of system resilience. Reliability Engineering and System Safety. 145: 47–61.

[6] PANTELI, M. y MANCARELLA, P. 2015. The Grid: Stronger, Bigger, Smarter? IEEE Power & Energy Magazine. 13(3): 58–66.

[7] BRUNEAU, M., CHANG, S., EGUCHI, R., LEE, G., O'ROURKE, T., REINHORN, A., SHINOZUKA, M., TIERNEY, K., WALLACE, W. y VON WINTERFELDT, D. 2003. A Framework to Quantitatively Assess and Enhance the Seismic Resilience of Communities. Earthquake Spectra. 19(4): 733–752.

[8] ZOBEL, C. 2010. Comparative Visualization of Predicted Disaster Resilience. The 7th International Conference on Information Systems for Crisis Response and Management (ISCRAM). (May): 1–6.

[9] BAZMI, A. y ZAHEDI, G. 2011. Sustainable energy systems: Role of optimization modeling techniques in power generation and supply—A review. Renewable and Sustainable Energy Reviews. 15(8): 3480–3500.

[10] VALENZUELA-VENEGAS, G. 2019. Design of sustainable and resilient eco-industrial parks by means of optimization tools. Universidad de Chile.

[11] VALENZUELA-VENEGAS, Guillermo, VERA-HOFMANN, Gabriela y DÍAZ-ALVARADO, Felipe A. 2020. Design of sustainable and resilient eco-industrial parks: Planning the flows integration network through multi-objective optimization. Journal of Cleaner Production [en línea]. 243. ISSN 09596526. 10.1016/j.jclepro.2019.118610

[12] ESPINOZA, S., SACAAN, R., RUDNICK, H., PANTELI, M., MANCARELLA, P., POULOS, A., DE LA LLERA, J., NAVARRO, A. y MORENO, R. 2018. Seismic resilience assessment and adaptation of the Northern Chilean power system. IEEE Power and Energy Society General Meeting. : 1–5.

[13] LAGOS G., T. 2017. Designing resilient power networks against natural hazards.

(October 2018).

[14] MORENO, S., HAAS, J., JUNNE, T., ELTROP, L. y VERA, G. 2018. A green copper concept: on the design of a full-renewable energy supply for its production. En: International Symposium on Energy System Optimization.

[15] BRUNEAU, M. y REINHORN, A. 2007. Exploring the concept of seismic resilience for acute care facilities. Earthquake Spectra. 23(1): 41–62.

[16] ZOBEL, C. 2011. Representing perceived tradeoffs in defining disaster resilience. Decision Support Systems. 50(2): 394–403.

[17] AFGAN, N. y VEZIROGLU, A. 2012. Sustainable resilience of hydrogen energy system. International Journal of Hydrogen Energy. 37(7): 5461–5467.

[18] ENJALBERT, S., VANDERHAEGEN, F., PICHON, M., OUEDRAOGO, K. y MILLOT, P. 2011. Human Modelling in Assisted Transportation. Human Modelling in Assisted Transportation. : 335–341.

[19] CHEN, L. y MILLER-HOOKS, E. 2011. Resilience: An Indicator of Recovery Capability in Intermodal Freight Transport. Transportation Science. 46(1): 109–123.

[20] FRANCHIN, P. y CAVALIERI, F. 2015. Probabilistic assessment of civil infrastructure resilience to earthquakes. Computer-Aided Civil and Infrastructure Engineering. 30(7): 583–600.

[21] ROSE, A. 2007. Economic resilience to natural and man-made disasters: Multidisciplinary origins and contextual dimensions. Environmental Hazards. 7(4): 383–398.

[22] OMER, M., NILCHIANI, R. y MOSTASHARI, A. 2009. Measuring the resilience of the global internet infrastructure system. 2009 IEEE International Systems Conference Proceedings. (November): 156–162.

[23] HENRY, D. y RAMIREZ-MARQUEZ, J. 2012. Generic metrics and quantitative approaches for system resilience as a function of time. Reliability Engineering and System Safety. 99: 114–122.

[24] BAROUD, H., RAMIREZ-MARQUEZ, J., BARKER, K. y ROCCO, C. 2014. Stochastic Measures of Network Resilience: Applications to Waterway Commodity Flows. Risk Analysis. 34(7): 1317–1335.

[25] BARKER, K. y RAMIREZ-MARQUEZ, J. 2016. Infrastructure Network Resilience. IRGC Resource Guide on Resilience. : 1–7.

[26] SHINOZUKA, M., FENG, M., KIM, H. y KIM, S. NONLINEAR STATIC PROCEDURE FOR FRAGILITY CURVE DEVELOPMENT. 2000.

[27] OMER, Mayada, NILCHIANI, Roshanak y MOSTASHARI, Ali. 2009. Measuring the resilience of the global internet infrastructure system. En: 2009 3rd Annual IEEE

Systems Conference [en línea]. IEEE, p. 156–162. ISBN 978-1-4244-3462-6. 10.1109/SYSTEMS.2009.4815790

[28] WHITMAN, R., ANAGNOS, T., KIRCHER, C., LAGORIO, H., LAWSON, R. y SCHNEIDER, P. 1997. Development of a national earthquake loss estimation methodology. Earthquake Spectra. 13(4): 643–661.

[29] KIRCHER, C., WHITMAN, R. y HOLMES, W. 2006. HAZUS Earthquake Loss Estimation Methods. Natural Hazards Review. 7(2): 45–59.

[30] KROESE, D., BRERETON, T., TAIMRE, T. y BOTEV, Z. 2014. Why the Monte Carlo method is so important today. Wiley Interdisciplinary Reviews: Computational Statistics. 6(6): 386–392.

[31] BURKE, Edmund K y KENDALL, Graham. 2014. Search Methodologies. ISBN 9781461469391.

[32] NOCEDAL, J. y WRIGHT, S. 2006. Numerical optimization. Springer. 664 p.

[33] ZITZLER, E. 1999. Evolutionary Algorithms for Multiobjective Optimization: Methods and Applications. Zurich. Swiss Federal Institute of Technology Zurich.

[34] HAAS, J., NOWAK, W. y PALMA-BEHNKE, R. 2019. Multi-objective planning of energy storage technologies for a fully renewable system: Implications for the main stakeholders in Chile. Energy Policy. 126: 494–506.

8. Nomenclature

8.1 Sets

$I = \{e, f, h\}$	Set of energy type:
e	Electricity
f	Fuel
h	Heat
D	Set of the process which demands energy.
TEC	Set of all technologies of the system.
$PG_i \subseteq TEC$	Set of primary generation technologies of the energy type $i \in I$.
$r1$	PV
$r2$	Wind Turbine
$rh1$	Flat Plate Collectors
$rh2$	CSP - Parabolic Trough
$TT_{i,j} \subseteq TEC$	Set of transformation technologies of the energy type $i \in I$ to energy type $j \in I$.
ptg	Electrolyzer
htp	CSP - Power Block
pth	Heating Rod
gtp	Fuel Cell.
$S_i \subseteq TEC$	Set of primary storage technologies of the energy type $i \in I$.
s	Li-Battery
sh	Hot Water Tank
$shht$	Molten Salts Storage

sf	H_2 Storage

$K = \{En, Ec, R\}$ Set of indicators:

En	Environmental
Ec	Economic
R	Resilience

8.2 Parameters

t_0	Time when the event occurs.
t_r	Reposition time.
T^*	Evaluation time.
E_d^i	Energy $i \in I$ demanded by process $d \in D$.
$D(t)$	Energy demand on time t.
D_T	Total energy demand.
$x_{b,tec}$	The fraction of damage of the technology $tec \in TEC$ for the process $b \in B$.
ω_k	Relative weight of the indicator k.

8.3 Variables

R	Resilience.	$[0,1]$
R^i	Resilience of the energy type $i \in I$.	$[0,1]$
R_T	Total resilience.	$[0,1]$
$Q(t)$	System health on time.	$\mathbb{R}^+ \cup \{0\}$
t	Time	$\mathbb{R}^+ \cup \{0\}$
$E_{d,gp}^i$	Generated energy $i \in I$ by technology $gp \in GP$ for the process $d \in D$.	$\mathbb{R}^+ \cup \{0\}$

$E^{i,j}{}_{d,tt}$	Transformed energy from type i to j by technology $tt \in TT$ for the process $d \in D$. $\{i,j\} \in I$.	$\mathbb{R}^+ \cup \{0\}$
$E^{i,in}_{d,a}$	Inflow energy $i \in I$ for technology $a \in A$ for the process $d \in D$.	$\mathbb{R}^+ \cup \{0\}$
$E^{i,out}_{d,a}$	Outflow energy $i \in I$ for technology $a \in A$ for the process $d \in D$.	$\mathbb{R}^+ \cup \{0\}$
$P(t)$	Generated power on time t	$\mathbb{R}^+ \cup \{0\}$
$P_{d,gp}(t)$	Generated power by technology $gp \in GP$ for the process $d \in D$ on time t.	$\mathbb{R}^+ \cup \{0\}$
$P_{d,tt}(t)$	Transformed power by technology $tt \in TT$ for the process $d \in D$ on time t.	$\mathbb{R}^+ \cup \{0\}$
$P^{in}_{d,a}(t)$	Inflow power of technology $a \in A$ for the process $d \in D$ on time t.	$\mathbb{R}^+ \cup \{0\}$
$P^{out}_{d,a}(t)$	Outflow power of technology $a \in A$ for the process $d \in D$ on time t.	$\mathbb{R}^+ \cup \{0\}$
$P^{inst}_{d,tec}$	Installed capacity of the technology $tec \in TEC$ for the process $d \in D$.	$\mathbb{R}^+ \cup \{0\}$
$P^{av}_{d,tec}(t)$	Available capacity of the technology $tec \in TEC$ for the process $d \in D$ on time t	$\mathbb{R}^+ \cup \{0\}$
ESh_i	Energy shortage of type $i \in I$	$\mathbb{R}$
ESh_i^+	Positive energy shortage of type $i \in I$	$\mathbb{R}^+\{0\}$
PSh_i	Power shortage of type $i \in I$	$\mathbb{R}$
PSh_i^+	Positive power shortage of type $i \in I$	$\mathbb{R}^+ \cup \{0\}$
OF	Objective function	$\mathbb{R}$

Appendixes

A. Appendix A: HAZUS Earthquake Model

The HAZUS Earthquake Model is designed to produce loss estimates for planning earthquake risk mitigation, emergency preparedness, response, and recovery. The methodology deals with nearly all aspects of the built environment, and a wide range of different types of losses. [4] To estimate the damage and predict the restoration of the components, the methodology uses two important concepts: fragility curves and restoration curves [28].

Fragility Curves

The fragility curves describe the probability of damage to a building, including structural systems and nonstructural components. Depending on the component response, fragility curves distribute damage between four physical damage states: slight, moderate, extensive, and complete [29].

Fragility curves used in HAZUS Model are lognormal probability functions that describe the likelihood of reaching, or exceeding structural and nonstructural damage states, given an estimate of peak building response. These curves consider the variability, including inherent uncertainty associated with capacity curve properties, damage states, and ground shaking (Usually measured as PGA) [29].

Fig. 21 illustrates the fragility curves for each damage state. For any given value PGA, discrete damage-state probabilities are calculated as the difference of the cumulative probabilities of reaching or exceeding successive damage states.

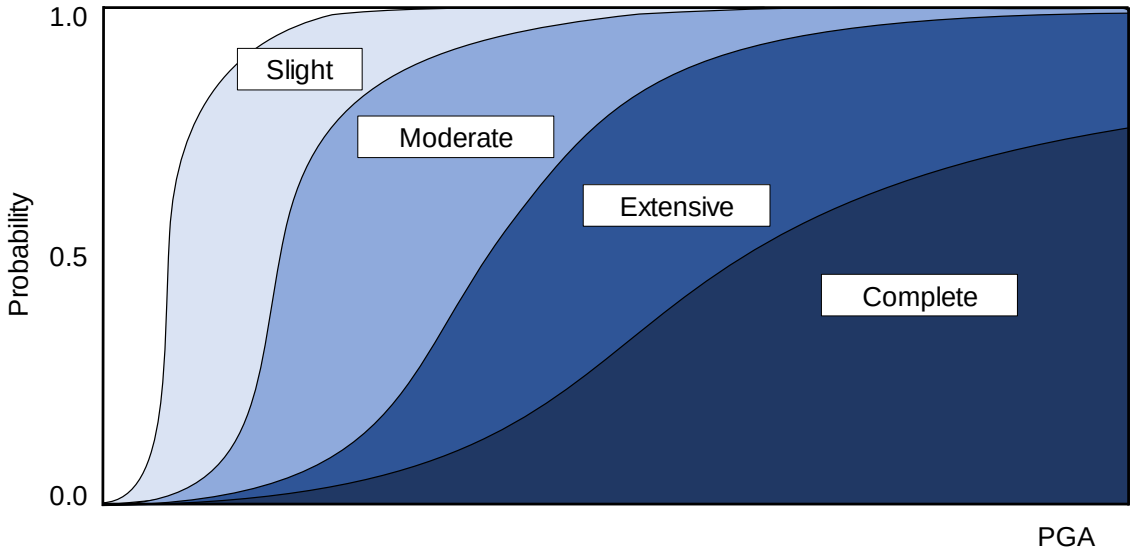

Fig. 21: Example fragility curves for slight, moderate, extensive and complete damage [29].

Restoration curves

Restoration curves describe the fraction or percentage of the system that is expected to be open or operational as a function of time following the earthquake. [4] This can be graphically represented as shown in Fig. 22, where the system health increase over time.

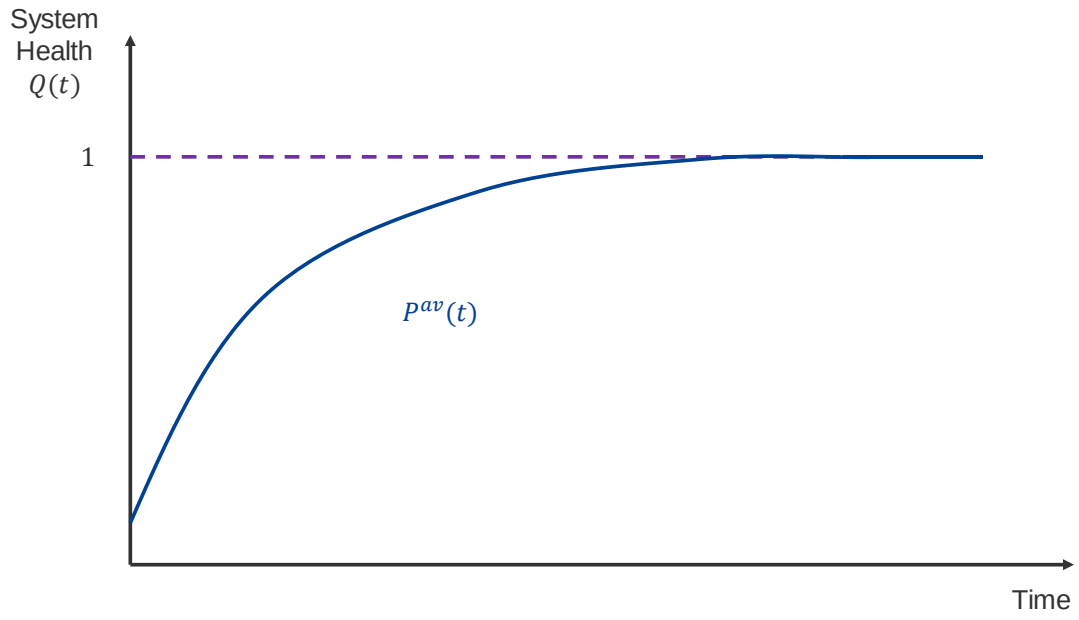

Fig. 22: Restoration curve: System health over time.

B. Appendix B: Monte Carlo Method

The essence of the Monte Carlo Method (MCM) is the generation of random objects or processes by means of a computer. These objects could arise 'naturally' as part of the modeling of a real-life system, apply to many fields such as physics, engineering, or economics. However, in many cases, the random objects in Monte Carlo techniques are introduced 'artificially' in order to solve deterministic problems. In this case, the MCM simply involves random sampling from certain probability distributions. Therefore, the idea of the Monte Carlo technique is to repeat the experiment many times to obtain several values of interest using the Law of Large Numbers and other methods of statistical inference. [30]

Some typical uses of MCM are sampling, estimation, and optimization. For this work, we focus on the latter. The MCM is a powerful tool for the optimization of complicated objective functions. In many applications these functions are deterministic, and randomness is introduced artificially in order to more efficiently search the domain of the objective function, as the case of this study. However, Monte Carlo techniques are also used to optimize noisy functions, where the function itself is random, for example, the result of a Monte Carlo simulation. [30]

C. Appendix C: Optimization Methods

Optimization is known as a tool to find the best possible solution given many available. To make use of this tool, we must find an objective, i.e. a function to represent a quality of a given solution and we use a search algorithm to minimize (or maximize) this objective [31].

Single-objective Optimization

Mathematically speaking, optimization is the minimization (or maximization) of an objective function subject to constraints in its variables. The optimization problem can be written as follows [32]:

$$\min_{x \in R^n} f(x)$$

$$subject\ to \quad c(x) = \big(c_1(x), c_2(x), \dots, c_n(x)\big) \leq 0 \qquad \text{(eq. 23)}$$

$$where \qquad x = (x_1, x_2, \dots, x_n) \in X$$

In this equation, x is the decision vector, f is the objective function, X is the decision space, and $c(x) \leq 0$ are the constrains, which determine the set of feasible solutions.

Multi-objective Optimization

Almost every real problem involves more than a single objective and often there are competing objectives. While in single-objective optimization problems (SOP) the optimal solution is usually clearly defined, this does not hold for multi-objective optimization problems (MOP). Instead of a single optimal solution, there is a set of alternative trade-offs among objectives [33].

A MOP is similar to a single-objective optimization (described in (eq. 23)), including variables (x), constraints (c), and a set of k objective functions (f) :

$$\min_{x \in R^n} f(x) = f_1(x), f_2(x), \dots, f_k(x)$$
$$subject\ to \quad c(x) = \big(c_1(x), c_2(x), \dots, c_n(x)\big) \leq 0 \qquad \text{(eq. 24)}$$

The set of alternative trade-offs can be graphically represented with the Pareto-optimal front, as is shown in Fig. 23, where the optimal points are in the Pareto-optimal front, which divide two regions: feasible region, where are the feasible solutions, and infeasible region, where solutions do not satisfy the constraint of the MOP [33].

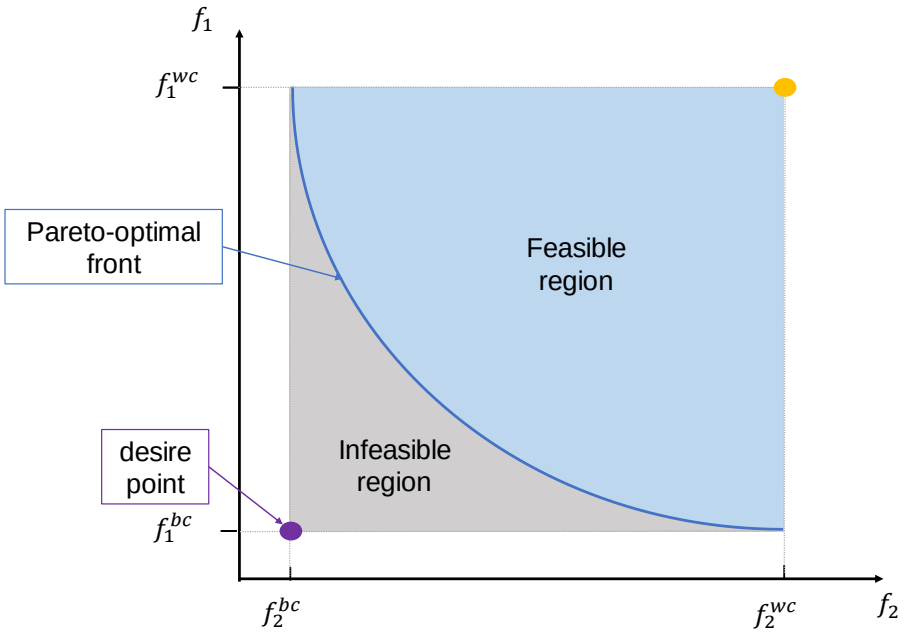

Fig. 23: Illustrative example of Pareto-optimal front.

Multi-objective Optimization Methods

There are several methods to solve a MOP. Usually, they aggregate the objectives into a single objective function. Some of the classical methods are the weighting method, the

constraint method, goal programming [33]. The two first mentioned are briefly described here.

Weighting Method

For the weighting method the MOP is converted to an SOP by a linear combination of the objectives [33]:

$$\min_{x \in R^n} f(x) = \omega_1 \cdot f_1(x) + \omega_2 \cdot f_2(x) + \ldots + \omega_k \cdot f_k(x)$$
$$subject\ to \quad c(x) = \left(c_1(x), c_2(x), \ldots, c_n(x)\right) \leq 0 \qquad \text{(eq. 25)}$$

ω_i are the weights of each function, and usually are normalized such that $\sum \omega_i = 1$.

The main disadvantage of this method is that it cannot generate all Pareto-optimal solutions with non-convex trade-off surfaces [33].

ε-Constraint Method

Another method that fixed the problem is the ε-constraint method, which transforms $k - 1$ of the k objectives into constraints. The remaining objective (f_h) is the objective function of the resulting SOP[33]:

$$\min_{x \in R^n} f(x) = f_h(x)$$
$$subject\ to \quad c_i(x) = f_i(x) \leq \epsilon_i, \quad (1 \leq i \leq k, i \neq h) \qquad \text{(eq. 26)}$$

The upper bounds ϵ_i, is the parameter that is varied to obtain multiple Pareto-optimal solutions.

This method is able to obtain solutions associated with non-convex parts of the trade-off curve. However, this technique has another problem. If the upper bounds are not appropriately chosen, the obtained feasible set might be empty. Therefore, the suitable range of values for the bounds must be known beforehand [33].

On the other hand, this method is difficult to give importance to each function, when we are generating the Pareto-optimal front.

Normalized Constraint Method

To solve the last-mentioned problem of the constraint method, we use a normalized method. Therefore, the upper and lower bounds must be known beforehand. This can be obtained by an SOP on each objective. The best case for each one of the h objectives is optimal for f_h ($f_i^{bc}(x)$), and the worst-case ($f_i^{wc}(x)$) is the maximum obtained value from the optimization of f_i, where $i \neq k$.

$$\min_{x \in R^n} f(x) = f_h(x)$$

$$subject\ to \quad c_i(x) = \frac{f_i(x) - f_i^{bc}(x)}{f_i^{wc}(x) - f_i^{bc}(x)} \leq \omega_i, \quad (1 \leq i \leq k, i \neq h) \qquad \text{(eq. 27)}$$

In the last equation, ω_i are the normalized weights of each function.

D. Appendix D: Installed Capacity of each Technology: Case Study

Table 7: The installed capacity of each technology case min costs.

Installed capacity (MW)	
r1	1649
r2	587
rh1	0
rh2	144
ptg	212
htp	0
pth	92
gtp	60
Converter size (MW)	
s	306
sh	92
shht	0
sf	203
Storage size (MWh)	
s	1916
sh	1515
shht	0

E. Appendix E: Fragility Curves

This appendix contains the date used to represent de damage of each technology for an event with PGA equal to 0.6g.

Data Obtained from HAZUS Methodology

Generation Facilities

This data is used for the following technologies: PV, Wind Turbine, Flat Collectors, CSP-Parabolic Trough, CSP-Power Block.

Table 8: Damage algorithms for generation facilities [4].

Damage state	Median (g)	β
Slight (ds_2)	0.1	0.5
Moderate (ds_3)	0.17	0.5
Extensive (ds_4)	0.42	0.5
Complete (ds_5)	0.58	0.55

Table 9: Restoration function for generation facilities [4].

Damage state	Mean (days)	β
Slight (ds_2)	0.5	0.1
Moderate (ds_3)	3.6	3.6
Extensive (ds_4)	22	21
Complete (ds_5)	65	30

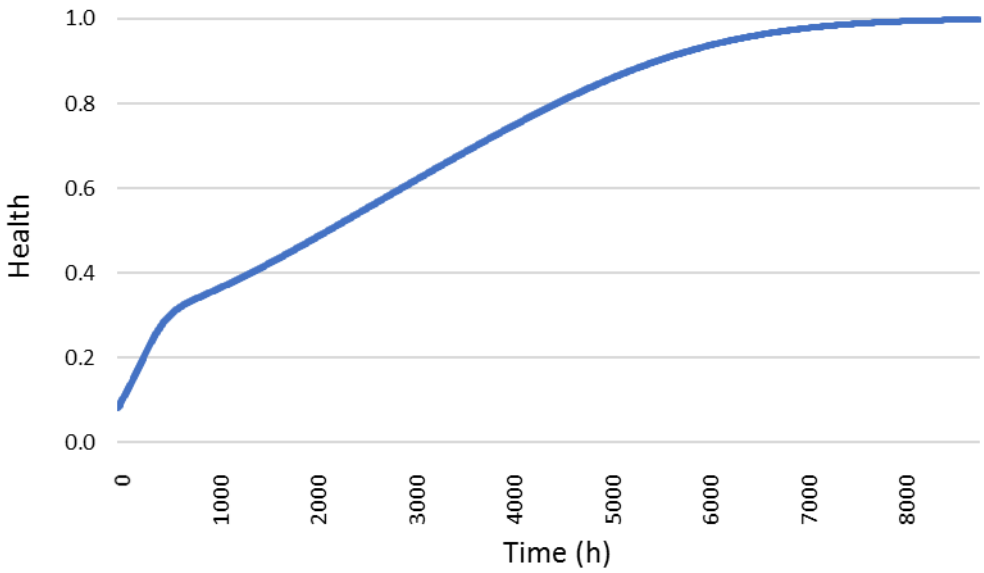

Fig. 24: Restoration curve for generation facilities.

Communication Facilities

This data is used for the following technologies: Battery, Fuel Cell, Electrolyzer [4].

Table 10: Damage algorithms for communication facilities [4].

Damage state	Median (g)	β
Slight (ds_2)	0.13	0.55
Moderate (ds_3)	0.26	0.5
Extensive (ds_4)	0.46	0.62
Complete (ds_5)	1.03	0.62

Table 11: Restoration function for communication facilities [4].

Damage state	Mean (days)	β
Slight (ds_2)	0	0.1
Moderate (ds_3)	0.5	0.2
Extensive (ds_4)	1	1
Complete (ds_5)	7	7

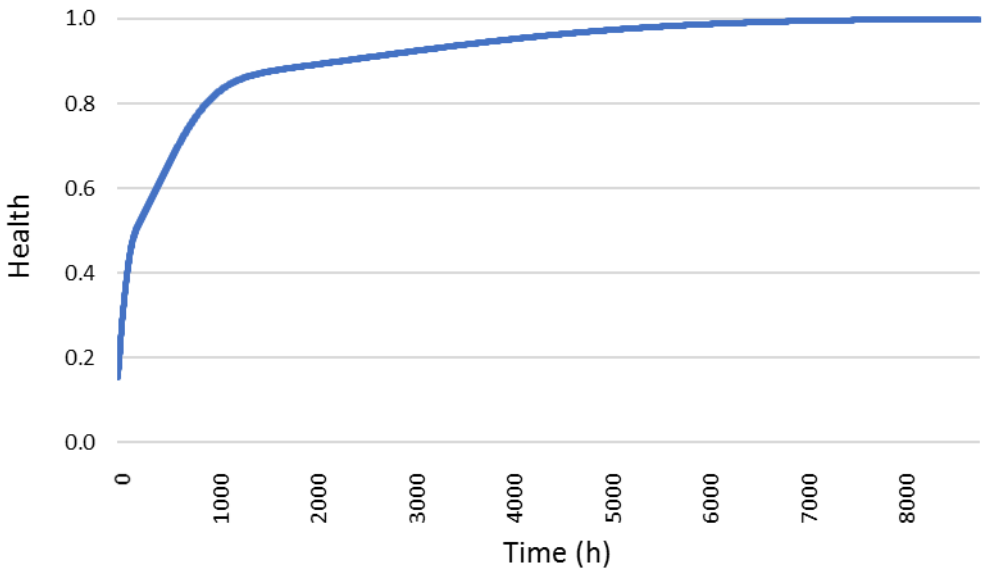

Fig. 25: Restoration curve for communication facilities.

Water Storage Tank

This data is used for the following technologies: Water Tank [4].

Table 12: Damage algorithms for water storage tank [4].

Damage state	Median (g)	β
Slight (ds_2)	0.15	0.7
Moderate (ds_3)	0.35	0.75
Extensive (ds_4)	0.68	0.75
Complete (ds_5)	0.95	0.7

Table 13: Restoration function for water storage tank [4].

Damage state	Mean (days)	β
Slight (ds_2)	1.2	0.4
Moderate (ds_3)	3.1	2.7
Extensive (ds_4)	93	85
Complete (ds_5)	155	120

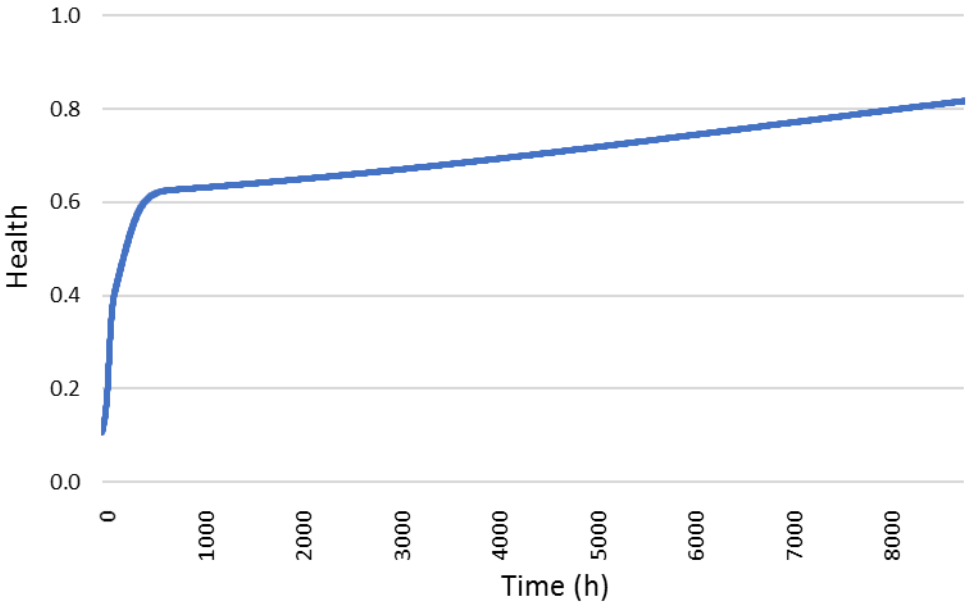

Fig. 26: Restoration curve for a water storage tank.

Storage Tanks

This data is used for the following technologies: Molten Salt Storage, H2 Storage [4].

Table 14: Damage algorithms for storage tank [4].

Damage state	Median (g)	β
Slight (ds_2)	0.3	0.6
Moderate (ds_3)	0.7	0.6
Extensive (ds_4)	1.25	0.65
Complete (ds_5)	1.6	0.6

Table 15: Restoration function for storage tank [4].

Damage state	Mean (days)	β
Slight (ds_2)	1.2	0.4
Moderate (ds_3)	3.1	2.7
Extensive (ds_4)	93	85
Complete (ds_5)	155	120

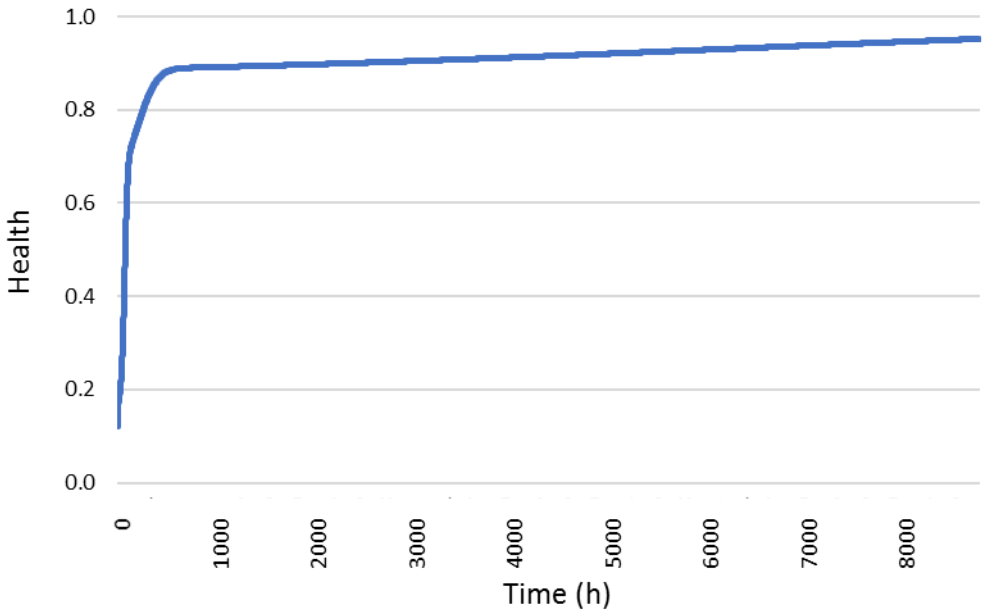

Fig. 27: Restoration curve for a storage tank.

Boiler

This data is used for the following technologies: Heating Rod [4].

Table 16: Damage algorithms for boilers [4].

Damage state	Median (g)	β
Slight (ds_2)	0.05	0.15
Moderate (ds_3)	0.4	0.4
Extensive (ds_4)	0.7	0.8
Complete (ds_5)	1	1.5

Table 17: Restoration function for boilers [4].

Damage state	Mean (days)	β
Slight (ds_2)	1.2	0.4
Moderate (ds_3)	3.1	2.7
Extensive (ds_4)	93	85
Complete (ds_5)	155	120

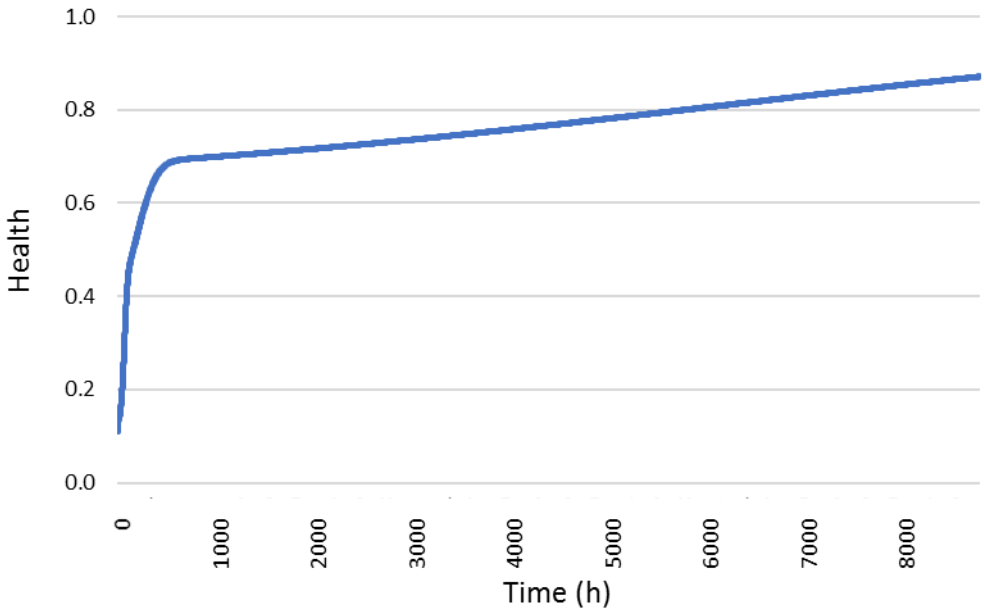

Fig. 28: Restoration curve for boilers.

Calculation Report

$$P[ds|s_d] = \Phi\left[\frac{1}{\beta}\ln\left(\frac{s_d}{s_{d,ds}}\right)\right] \quad \text{(eq. 28)}$$

Where Φ is the standard normal distribution.

$$\Phi(z) = \frac{1}{\sqrt{2\pi}}\int_{-\infty}^{z} e^{\frac{u^2}{2}}du \quad \text{(eq. 29)}$$

And,

$$z = \frac{1}{\beta}\ln\left(\frac{s_d}{s_{d,ds}}\right) \quad \text{(eq. 30)}$$

And finally, the probability for the different damage state is:

$$FR_{ds}(t) = \Phi_{\mu,\beta}(x) = \frac{1}{\beta\sqrt{2\pi}} \int_{-\infty}^{x} e^{\frac{(u-\mu)^2}{2\beta^2}} du \qquad \text{(eq. 31)}$$

Therefore, the functionality is

$$FP_{ds}(t) = P_{ds} \cdot FR_{ds}(t) = 0.01 \qquad \text{(eq. 32)}$$

For example, for the generation facilities (data in 0), given a PGA equal to 0.6, for slight damage:

$$z = \frac{1}{0.5} \ln\left(\frac{0.6}{0.1}\right) = 3.58 \qquad \text{(eq. 33)}$$

$$\Phi(3.58) = \frac{1}{\sqrt{2\pi}} \int_{-\infty}^{3.58} e^{\frac{u^2}{2}} du = 1.00 \qquad \text{(eq. 34)}$$

We do the same procedure for each damage state. The results are given in the following table:

Table 18: Probabilities for different damage state for generation facilities.

Damage state	Φ	P_{ds}
None (ds_1)	1.00	0.00
Slight (ds_2)	1.00	0.01
Moderate (ds_3)	0.99	0.23
Extensive (ds_4)	0.76	0.24
Complete (ds_5)	0.52	0.52

To estimate the functionality for each restoration period, we use (eq. 31). For example, for slight damage after 10 days:

$$FR_{ds_2}(t = 10) = \frac{1}{0.1\sqrt{2\pi}} \int_{-\infty}^{10} e^{\frac{(u-0.5)^2}{2 \cdot 0.1^2}} du = 1.00 \qquad \text{(eq. 35)}$$

And the estimate of functionality is:

$$FP_{ds_2}(t = 10) = P_{ds_2} \cdot FR_{ds_2} = 0.01 \quad \text{(eq. 36)}$$

For each damage state, after 10 days, the functionality is given in the following table:

Table 19: Restoration period and functionality for each damage state for generation facilities after 10 days.

Damage state	FR	FP
None (ds_1)	1.00	0.00
Slight (ds_2)	1.00	0.01
Moderate (ds_3)	0.54	0.13
Extensive (ds_4)	0.20	0.05
Complete (ds_5)	0.02	0.01
Total		0.19

Therefore, given a PGA equal to 0.6, after 10 days about the power generation will be about 19% of the initial value.

We can graph the functionality of the technology for each time as it is shown in Fig. 24.

F. Appendix F: Results of Three Scenarios

Install Capacity of each Technology

Table 20: The installed capacity of each technology for the three scenarios.

	$\boldsymbol{min\ Cost}$	$\boldsymbol{50\%\ Re-Co}$	$\boldsymbol{max\ Re}$
	Installed capacity (MW)		
r1	1649	1455	1136
r2	587	24	6
rh1	0	0	0
rh2	144	76	137
ptg	212	238	179
htp	0	0	6
pth	92	94	25
gtp	60	33	7
	Converter size (MW)		
s	306	355	499
sh	92	94	33
shht	0	0	96
sf	203	194	135

	Storage size (MWh)		
s	1916	2128	2499
sh	1515	873	747
shht	0	0	540
sf	21921	4570	5214

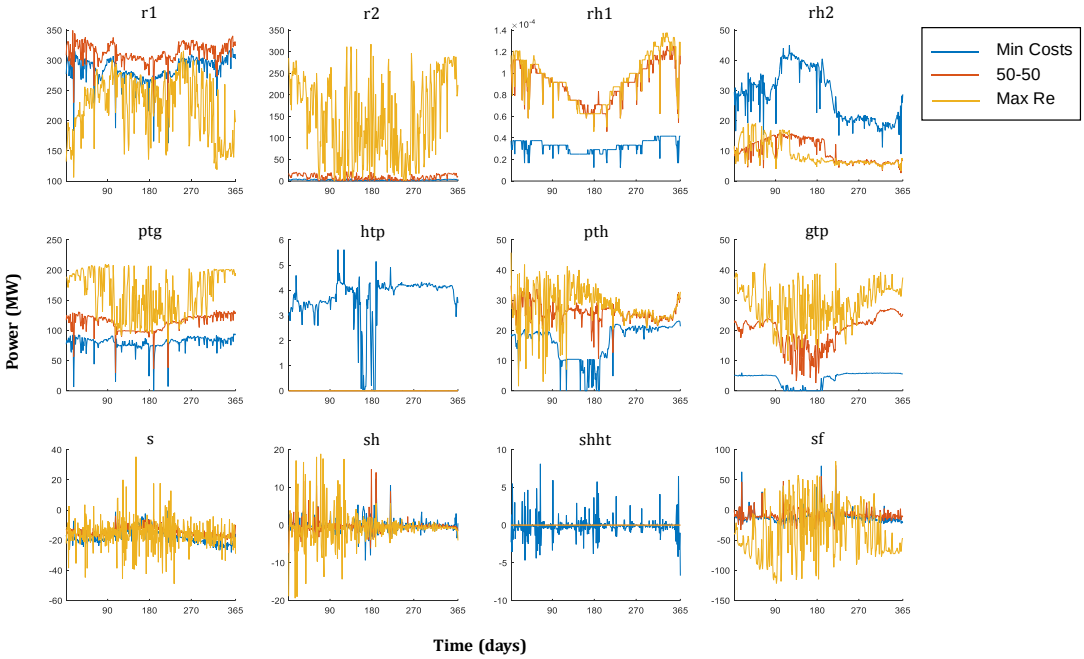

Fig. 29: Performance of each technology over time for the three scenarios. For the storage, the negative values represent the charge and positive values discharge.

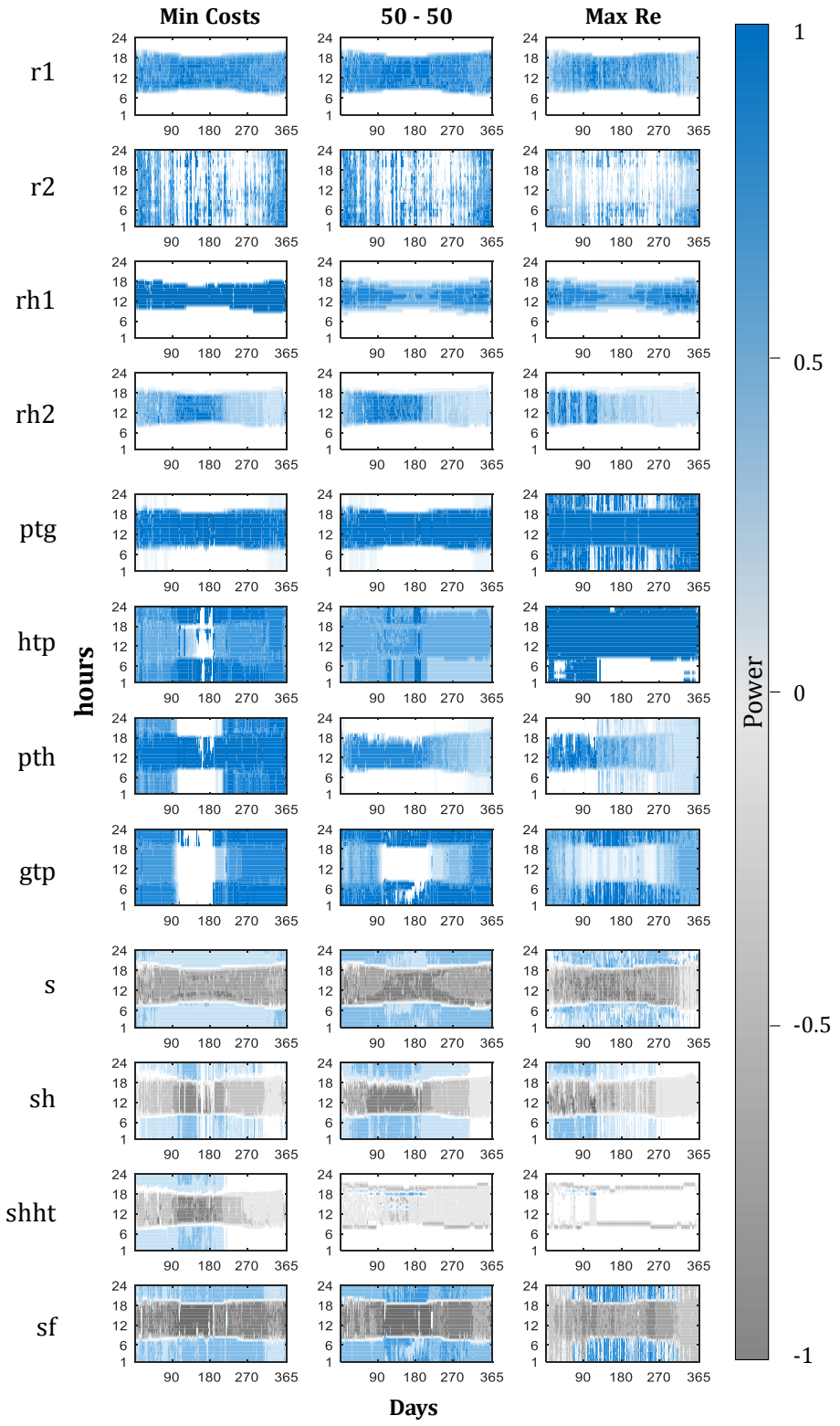

Fig. 30: Performance of each technology over time for three scenarios. The X-axis shows the days of the year and the Y-axis shows the hours of the day. The power is normalized by the maximum value for each technology. For the storage, the negative values represent the charge and positive values discharge.

G. Appendix G: Model Formulation

This appendix shows the complete model formulation used for this thesis adapted from the work of [14] and [34]. First, we present the nomenclature of the sets, parameters and variables used, then the general equations and finally, the specific equations and OF for the different models.

Sets

D	Set of the process which demands energy.
T	Time
TEC	Set of all technologies of the system.
$PG \subseteq TEC$	Set of primary generation technologies of the energy type $i \in I$.
$r1$	PV
$r2$	Wind Turbine
$rh1$	Flat Plate Collectors
$rh2$	CSP - Parabolic Trough
$TT_{i,j} \subseteq TEC$	Set of transformation technologies of the energy type $i \in I$ to energy type $j \in I$.
ptg	Electrolyzer
htp	CSP - Power Block
pth	Heating Rod
gtp	Fuel Cell.
$S_i \subseteq TEC$	Set of primary storage technologies of the energy type $i \in I$.
se	Li-Battery
sh	Hot Water Tank
$shht$	Molten Salts Storage
sf	H_2 Storage

Parameters

η_{tt}	Efficiency of transformation technologies.
η_s^{load}	Energy load efficiency of storage technologies.
η_s^{unload}	Energy unload efficiency of storage technologies.
ω_{Re}	Relative weight of the resilience OF.
$annuity_{tec}$	Annuity of technology $tec \in TEC$.
$cost_{tec}^{op}$	Operational cost of technology $tec \in TEC$.
$cost_s^{op,load}$	Operational cost of loading $s \in S$.
$cost_s^{op,unload}$	Operational cost of unloading $s \in S$.
$cost_{tec}^{fix}$	Fixed operational cost of technology $tec \in TEC$.
$cost_s^{fix,cap}$	Fixed operational cost of technology $s \in S$ per volume.
$cost_s^{fix,conv}$	Fixed operational cost of technology $s \in S$ per conversion.
$cost_{tec}^{inv}$	Investment cost of technology $tec \in TEC$.
$cost_s^{inv,cap}$	Investment cost of technology $s \in S$ per volume.
$cost_s^{inv,conv}$	Investment cost of technology $s \in S$ per conversion.
$Demand_{t,d}^{e}$	Electricity demand for process $d \in D$ during time $t \in T$.
$Demand_{t,d}^{h}$	Heat demand for process $d \in D$ during time $t \in T$.
$Demand_{t,d}^{f}$	Fuel demand for process $d \in D$ during time $t \in T$.
$Demand^{total}$	Total demand for the system.
$E_{d,tec}^{inst}$	Installed capacity of technology $tec \in TEC$ for process $d \in D$ (for operational simulation).
$E_{d,s}^{inst,cap}$	Installed volume capacity of technology $s \in S$ for process $d \in D$ (for operational simulation).

$E_{d,s}^{inst,conv}$	Installed converters capacity of technology $s \in S$ for process $d \in D$ (for operational simulation).
$losses_s$	Energy losses over time for technology $s \in S$.
$Profile_{t,d,pg}$	Profile of renewable technologies $pg \in PG$ of process $d \in D$ during time $t \in T$.
Re^{max}	Maximum resilience value.
Re^{min}	Minimum resilience value.
$ReCurve_{t,d,tec}$	Restoration curve for technology $tec \in TEC$ of process $d \in D$ during time $t \in T$.
$ReTime_{t,d,tec}$	Restoration function for MC simulation (step-function) for technology $tec \in TEC$ of process $d \in D$ during time $t \in T$.
$YearFraction$	Fraction of the year simulated.

Variables

$Costs^{fix,tec}$	Fixed operational costs of technology $tec \in TEC$.	$\mathbb{R}^+ \cup \{0\}$
$Costs^{inv,tec}$	Investment costs of technology $tec \in TEC$.	$\mathbb{R}^+ \cup \{0\}$
$Costs^{inv,total}$	Total investment costs.	$\mathbb{R}^+ \cup \{0\}$
$Costs^{op,tec}$	Fixed operational costs of technology $tec \in TEC$.	$\mathbb{R}^+ \cup \{0\}$
$Costs^{op,total}$	Total operational costs.	$\mathbb{R}^+ \cup \{0\}$
$Costs^{total}$	Total costs.	$\mathbb{R}^+ \cup \{0\}$
$E_{d,tec}$	Installed capacity of technology $tec \in TEC$ for process $d \in D$.	$\mathbb{R}^+ \cup \{0\}$
$E_{d,s}^{cap}$	Installed volume capacity of technology $s \in S$ for process $d \in D$.	$\mathbb{R}^+ \cup \{0\}$
$E_{d,s}^{conv}$	Installed converters capacity of technology $s \in S$ for process $d \in D$.	$\mathbb{R}^+ \cup \{0\}$

$E_{d,s}^{first}$	Energy stored by $s \epsilon S$ for process $d \epsilon D$ during time $t = 1$.	$\mathbb{R}^+ \cup \{0\}$
$E_{d,s}^{last}$	Energy stored by $s \epsilon S$ for process $d \epsilon D$ during time $t = end$.	$\mathbb{R}^+ \cup \{0\}$
$E_{t,d,s}^{loss}$	Energy losses by $s \epsilon S$ for process $d \epsilon D$ during time $t \epsilon T$.	$\mathbb{R}^+ \cup \{0\}$
$E_{t,d,s}^{stored}$	Energy stored by $s \epsilon S$ for process $d \epsilon D$ during time $t \epsilon T$.	$\mathbb{R}^+ \cup \{0\}$
$E'^{loss}_{t,d,s}$	Energy losses by $s \epsilon S$ for process $d \epsilon D$ during time $t \epsilon T$ (auxiliary variable for resilience indicator).	$\mathbb{R}^+ \cup \{0\}$
$E'^{stored}_{t,d,s}$	Energy stored by $s \epsilon S$ for process $d \epsilon D$ during time $t \epsilon T$ (auxiliary variable for resilience indicator).	$\mathbb{R}^+ \cup \{0\}$
ESh_t^e	Energy shortage of electricity during time $t \epsilon T$.	$\mathbb{R}$
ESh_t^h	Energy shortage of heat during time $t \epsilon T$.	$\mathbb{R}$
ESh_t^f	Energy shortage of fuel during time $t \epsilon T$.	$\mathbb{R}$
ESh_t^{+e}	Positive energy shortage of electricity during time $t \epsilon T$.	$\mathbb{R}^+ \cup \{0\}$
ESh_t^{+h}	Positive energy shortage of heat during time $t \epsilon T$.	$\mathbb{R}^+ \cup \{0\}$
ESh_t^{+f}	Positive energy shortage of fuel during time $t \epsilon T$.	$\mathbb{R}^+ \cup \{0\}$
$P_{t,d,tec}$	Power delivered or transformed by $tec \epsilon TEC$ for process $d \epsilon D$ during time $t \epsilon T$.	$\mathbb{R}^+ \cup \{0\}$
$P_{t,d,s}^{load}$	Power stored by $s \epsilon S$ for process $d \epsilon D$ during time $t \epsilon T$.	$\mathbb{R}^+ \cup \{0\}$
$P_{t,d,s}^{unload}$	Power delivered by $s \epsilon S$ for process $d \epsilon D$ during time $t \epsilon T$.	$\mathbb{R}^+ \cup \{0\}$
$P_{t,d}^{tec1,tec2}$	Power delivered from $tec1 \epsilon TEC$ to $tec1 \epsilon TEC$ for process $d \epsilon D$ during time $t \epsilon T$.	$\mathbb{R}^+ \cup \{0\}$
$P_{t,d}^{unserved,e}$	Electricity unserved for process $d \epsilon D$ during time $t \epsilon T$.	$\mathbb{R}^+ \cup \{0\}$

$P_{t,d}^{unserved,h}$	Heat unserved for process $d \epsilon D$ during time $t \epsilon T$.	$\mathbb{R}^+ \cup \{0\}$
$P_{t,d}^{unserved,f}$	Fuel unserved for process $d \epsilon D$ during time $t \epsilon T$.	$\mathbb{R}^+ \cup \{0\}$
$P'_{t,d,tec}$	Power delivered or transformed by $tec \epsilon TEC$ for process $d \epsilon D$ during time $t \epsilon T$ (auxiliary variable for resilience indicator).	$\mathbb{R}^+ \cup \{0\}$
$P'^{load}_{t,d,s}$	Power stored by $s \epsilon S$ for process $d \epsilon D$ during time $t \epsilon T$ (auxiliary variable for resilience indicator).	$\mathbb{R}^+ \cup \{0\}$
$P'^{unload}_{t,d,s}$	Power delivered by $s \epsilon S$ for process $d \epsilon D$ during time $t \epsilon T$(auxiliary variable for resilience indicator).	$\mathbb{R}^+ \cup \{0\}$
$P'^{tec1,tec2}_{t,d}$	Power delivered from $tec1 \epsilon TEC$ to $tec1 \epsilon TEC$ for process $d \epsilon D$ during time $t \epsilon T$ (auxiliary variable for resilience indicator).	$\mathbb{R}^+ \cup \{0\}$
Re^e	Resilience value for electricity vector.	$[0,1]$
Re^h	Resilience value for heat vector.	$[0,1]$
Re^f	Resilience value for fuel vector.	$[0,1]$
Re^{total}	Total resilience.	$[0,1]$

General Equations

Operational costs

$$Costs^{op,pg} = \sum_t \sum_d \sum_{pg} \left(cost_{pg}^{op} \cdot P_{t,d,pg} \right) \quad \text{(eq. 37)}$$

$$Costs^{op,tt} = \sum_t \sum_d \sum_{tt} \left(cost_{tt}^{op} \cdot P_{t,d,tt} \right) \quad \text{(eq. 38)}$$

$$Costs^{op,s} = \sum_t \sum_d \sum_s \left(cost_s^{op,load} \cdot P_{t,d,s}^{load} + cost_s^{op,unload} \cdot P_{t,d,s}^{unload} \right) \quad \text{(eq. 39)}$$

Fixed operational costs

$$Costs^{fix,pg} = \sum_{d} \sum_{pg} \left(cost_{pg}^{fix} \cdot E_{d,pg} \right) \quad \text{(eq. 40)}$$

$$Costs^{fix,tt} = \sum_{d} \sum_{tt} \left(cost_{tt}^{fix} \cdot E_{d,tt} \right) \quad \text{(eq. 41)}$$

$$Costs^{fix,s} = \sum_{d} \sum_{s} \left(cost_{s}^{fix,cap} \cdot E_{d,s}^{cap} + cost_{s}^{fix,conv} \cdot E_{d,s}^{conv} \right) \quad \text{(eq. 42)}$$

Total operational costs

$$Costs^{op,total} = Costs^{op,pg} + Costs^{op,tt} + Costs^{op,s} + Costs^{fix,pg} + Costs^{fix,tt} + Costs^{fix,s} \quad \text{(eq. 43)}$$

Investment costs

$$Costs^{inv,pg} = \sum_{d} \sum_{pg} \left(annuity_{pg} \cdot cost_{pg}^{inv} \cdot E_{d,pg} \right) \quad \text{(eq. 44)}$$

$$Costs^{inv,tt} = \sum_{d} \sum_{tt} \left(annuity_{tt} \cdot cost_{tt}^{inv} \cdot E_{d,tt} \right) \quad \text{(eq. 45)}$$

$$Costs^{inv,s} = \sum_{d} \sum_{s} \left(annuity_{s} \cdot \left(cost_{s}^{inv,cap} \cdot E_{d,s}^{cap} + cost_{s}^{inv,conv} \cdot E_{d,s}^{conv} \right) \right) \quad \text{(eq. 46)}$$

Total investment costs

$$Costs^{inv,total} = YearFraction \cdot \left(Costs^{inv,pg} + Costs^{inv,tt} + Costs^{inv,s} \right) \quad \text{(eq. 47)}$$

Total costs

$$Costs^{total} = Costs^{op,total} \cdot Costs^{inv,total} \quad \text{(eq. 48)}$$

Energy balances

Maximum power constraint by the capacity

$$P_{t,d,pg} \leq E_{d,pg} \cdot Profile_{t,d,pg} \quad \forall t \epsilon T, d \epsilon D, pg \epsilon PG \quad \text{(eq. 49)}$$

$$P_{t,d,tt} \leq E_{d,tt} \quad \forall t \epsilon T, d \epsilon D, tt \epsilon TT \quad \text{(eq. 50)}$$

$$P_{t,d,s}^{load} \leq E_{d,s} \quad \forall t \epsilon T, d \epsilon D, s \epsilon S \quad \text{(eq. 51)}$$

$$P_{t,d,s}^{unload} \leq E_{d,s} \quad \forall t \epsilon T, d \epsilon D, s \epsilon S \quad \text{(eq. 52)}$$

$$P_{t,d,s}^{unload} \leq E_{d,s} \quad \forall t \epsilon T, d \epsilon D, s \epsilon S \quad \text{(eq. 53)}$$

Efficiency of transformation technologies

$$P_{t,d,htp} = P_{t,d}^{shht,htp} \cdot \eta_{htp} \quad \forall t \epsilon T, d \epsilon D \quad \text{(eq. 54)}$$

$$P_{t,d,gtp} = P_{t,d}^{sf,gtp} \cdot \eta_{gtp} \quad \forall t \epsilon T, d \epsilon D \quad \text{(eq. 55)}$$

Energy balances

$$P_{t,d,rh1} = P_{t,d}^{rh1,d} + P_{t,d}^{rh1,sh} \quad \forall t \epsilon T, d \epsilon D \quad \text{(eq. 56)}$$

$$P_{t,d,rh2} = P_{t,d}^{rh2,d} + P_{t,d}^{rh2,shht} \quad \forall t \epsilon T, d \epsilon D \quad \text{(eq. 57)}$$

$$P_{t,d,pth} = P_{t,d}^{pth,sh} + P_{t,d}^{pth,d} \quad \forall t \epsilon T, d \epsilon D \quad \text{(eq. 58)}$$

$$P_{t,d,ptg} = P_{t,d}^{ptg,sf} + P_{t,d}^{ptg,d} \quad \forall t \epsilon T, d \epsilon D \quad \text{(eq. 59)}$$

$$P_{t,d,sh}^{load} = P_{t,d}^{rh1,sh} + P_{t,d}^{pth,sh} \quad \forall t \epsilon T, d \epsilon D \tag{eq. 60}$$

$$P_{t,d,shht}^{unload} = P_{t,d}^{shht,d} + P_{t,d}^{shht,htp} \quad \forall t \epsilon T, d \epsilon D \tag{eq. 61}$$

$$P_{t,d,sf}^{unload} = P_{t,d}^{sf,gtp} + P_{t,d}^{sf,d} \quad \forall t \epsilon T, d \epsilon D \tag{eq. 62}$$

Energy balances in storage technologies

$$E_{t+1,d,s}^{stored} = E_{t,d,s}^{stored} - E_{t,d,s}^{loss} + \eta_s^{load} \cdot P_{t,d,s}^{load} - \frac{P_{t,d,s}^{unload}}{\eta_s^{unload}} \quad \forall t \epsilon T, d \epsilon D, s \epsilon S \tag{eq. 63}$$

$$E_{t,d,s}^{loss} = E_{t,d,s}^{stored} \cdot losses_s \quad \forall t \epsilon T, d \epsilon D, s \epsilon S \tag{eq. 64}$$

$$E_{t_{first},d,s}^{stored} = E_{d,s}^{first} \quad \forall d \epsilon D, s \epsilon S \tag{eq. 65}$$

$$E_{t_{last},d,s}^{stored} = E_{d,s}^{last} \quad \forall d \epsilon D, s \epsilon S \tag{eq. 66}$$

$$E_{d,s}^{first} = E_{d,s}^{last} \quad \forall d \epsilon D, s \epsilon S \tag{eq. 67}$$

Maximum storage energy capacities

$$E_{t,d,s}^{stored} \leq E_{d,s}^{cap} \quad \forall t \epsilon T, d \epsilon D, tt \epsilon TT \tag{eq. 68}$$

Satisfy demand

$$Demand_{t,d}^{e} = P_{t,d,r1} + P_{t,d,r2} + P_{t,d,htp} - \frac{P_{t,d,pth}}{\eta_{pth}} + P_{t,d,gtp} - \frac{P_{t,d,ptg}}{\eta_{ptg}} - P_{t,d,se}^{load} + P_{t,d,se}^{unload} + P_{t,d}^{unserved,e} \quad \forall t \epsilon T, d \epsilon D \tag{eq. 69}$$

$$Demand_{t,d}^{h} = P_{t,d,rh1} + P_{t,d,rh2} + P_{t,d}^{pth,d} + P_{t,d}^{shht,d} + P_{t,d,sh}^{unload} + P_{t,d}^{unserved,h} \quad \forall t \epsilon T, d \epsilon D \tag{eq. 70}$$

$$Demand_{t,d}^{f} = P_{t,d}^{ptg,d} + P_{t,d}^{sf,d} + P_{t,d}^{unserved,h} \quad \forall t \epsilon T, d \epsilon D \tag{eq. 71}$$

Operational Simulation Model with Restoration Curves

Maximum power available

$$E_{t,d,pg} \leq ReCurve_{t,d,pg} \cdot E_{d,pg}^{inst} \cdot profile_{t,d,pg} \quad \forall t \epsilon T, d \epsilon D, pg \epsilon PG \tag{eq. 72}$$

$$P_{t,d,tt} \leq ReCurve_{t,d,tt} \cdot E_{d,tt}^{inst} \quad \forall t \epsilon T, d \epsilon D, tt \epsilon TT \tag{eq. 73}$$

$$P_{t,d,s}^{load} \leq ReCurve_{t,d,s} \cdot E_{d,s}^{inst,conv} \quad \forall t \epsilon T, d \epsilon D, s \epsilon S \tag{eq. 74}$$

$$P_{t,d,s}^{unload} \leq ReCurve_{t,d,s} \cdot E_{d,s}^{inst,conv} \quad \forall t \epsilon T, d \epsilon D, s \epsilon S \tag{eq. 75}$$

$$P_{t,d,s}^{stored} \leq ReCurve_{t,d,s} \cdot E_{d,s}^{inst,cap} \quad \forall t \epsilon T, d \epsilon D, s \epsilon S \tag{eq. 76}$$

Resilience metric

$$Re^{e} = 1 - \sum_{t} \sum_{d} \frac{P_{t,d}^{unserved,e}}{Demand_{t,d}^{e}} \tag{eq. 77}$$

$$Re^{h} = 1 - \sum_{t} \sum_{d} \frac{P_{t,d}^{unserved,h}}{Demand_{t,d}^{h}} \tag{eq. 78}$$

$$Re^{f} = 1 - \sum_{t} \sum_{d} \frac{P_{t,d}^{unserved,f}}{Demand_{t,d}^{f}} \tag{eq. 79}$$

$$Re^{total} = \frac{Re^{e} \cdot Demand^{e} + Re^{h} \cdot Demand^{h} + Re^{f} \cdot Demand^{f}}{Demand^{total}} \quad \text{(eq. 80)}$$

Objective function

$$\min \sum_{t} \sum_{d} \left(P_{t,d}^{unserved,e} + P_{t,d}^{unserved,h} + P_{t,d}^{unserved,f} \right) \quad \text{(eq. 81)}$$

Monte Carlo Simulation Model

Maximum power available

$$P_{t,d,pg} \leq ReTime_{t,d,pg} \cdot E_{d,pg}^{inst} \cdot profile_{t,d,pg} \quad \forall t \epsilon T, d \epsilon D, pg \epsilon PG \quad \text{(eq. 82)}$$

$$P_{t,d,tt} \leq ReTime_{t,d,tt} \cdot E_{d,tt}^{inst} \quad \forall t \epsilon T, d \epsilon D, tt \epsilon TT \quad \text{(eq. 83)}$$

$$P_{t,d,s}^{load} \leq ReTime_{t,d,s} \cdot E_{d,s}^{inst,conv} \quad \forall t \epsilon T, d \epsilon D, s \epsilon S \quad \text{(eq. 84)}$$

$$P_{t,d,s}^{unload} \leq ReTime_{t,d,s} \cdot E_{d,s}^{inst,conv} \quad \forall t \epsilon T, d \epsilon D, s \epsilon S \quad \text{(eq. 85)}$$

$$E_{t,d,s}^{stored} \leq ReTime_{t,d,s} \cdot E_{d,s}^{inst,cap} \quad \forall t \epsilon T, d \epsilon D, s \epsilon S \quad \text{(eq. 86)}$$

Resilience metric

$$Re^{e} = 1 - \frac{\sum_{t} \sum_{d} P_{t,d}^{unserved,e}}{Demand^{e}} \quad \text{(eq. 87)}$$

$$Re^{h} = 1 - \frac{\sum_{t} \sum_{d} P_{t,d}^{unserved,h}}{Demand^{h}} \quad \text{(eq. 88)}$$

$$Re^{f} = 1 - \frac{\sum_{t} \sum_{d} P_{t,d}^{unserved,f}}{Demand^{f}} \quad \text{(eq. 89)}$$

$$Re^{total} = \frac{Re^{e} \cdot Demand^{e} + Re^{h} \cdot Demand^{h} + Re^{f} \cdot Demand^{f}}{Demand^{total}} \quad \text{(eq. 90)}$$

Objective function

$$\min \sum_{t} \sum_{d} \left(P_{t,d}^{unserved,e} + P_{t,d}^{unserved,h} + P_{t,d}^{unserved,f} \right) \quad \text{(eq. 91)}$$

Resilience Indicator

Maximum power available (auxiliary functions)

$$P'_{t,d,tec} \leq E_{t,d,tec} \quad \forall t \epsilon T, d \epsilon D, tec \epsilon TEC \quad \text{(eq. 92)}$$

$$P'_{t,d,pg} \leq ReCurve_{t,d,pg} \cdot E_{d,pg} \cdot profile_{t,d,pg} \quad \forall t \epsilon T, d \epsilon D, pg \epsilon PG \quad \text{(eq. 93)}$$

$$P'_{t,d,tt} \leq ReCurve_{t,d,tt} \cdot E_{d,tt} \quad \forall t \epsilon T, d \epsilon D, tt \epsilon TT \quad \text{(eq. 94)}$$

$$P'^{load}_{t,d,s} \leq ReCurve_{t,d,s} \cdot E_{d,s}^{conv} \quad \forall t \epsilon T, d \epsilon D, s \epsilon S \quad \text{(eq. 95)}$$

$$P'^{unload}_{t,d,s} \leq ReCurve_{t,d,s} \cdot E_{d,s}^{conv} \quad \forall t \epsilon T, d \epsilon D, s \epsilon S \quad \text{(eq. 96)}$$

$$P'^{stored}_{t,d,s} \leq ReCurve_{t,d,s} \cdot E_{d,s}^{cap} \quad \forall t \epsilon T, d \epsilon D, s \epsilon S \quad \text{(eq. 97)}$$

Energy balances in storage technologies (auxiliary functions)

$$E'^{stored}_{t+1,d,s} = E'^{stored}_{t,d,s} - E'^{loss}_{t,d,s} + \eta_{s}^{load} \cdot P'^{load}_{t,d,s} - \frac{P'^{unload}_{t,d,s}}{\eta_{s}^{unload}} \quad \forall t \epsilon T, d \epsilon D, s \epsilon S \quad \text{(eq. 98)}$$

$$E'^{loss}_{t,d,s} = E'^{stored}_{t,d,s} \cdot losses_{s} \quad \forall t \epsilon T, d \epsilon D, s \epsilon S \quad \text{(eq. 99)}$$

$$E'^{stored}_{t_{first},d,s} \leq E^{stored}_{t_{first},d,s} \quad \forall d \epsilon D, s \epsilon S \quad \text{(eq. 100)}$$

$$E'^{stored}_{t_{last},d,s} \leq E^{stored}_{t_{last},d,s} \quad \forall d \epsilon D, s \epsilon S \tag{eq. 101}$$

Energy balances

$$P'_{t,d,rh1} = P'^{rh1,d}_{t,d} + P'^{rh1,sh}_{t,d} \quad \forall t \epsilon T, d \epsilon D \tag{eq. 102}$$

$$P'_{t,d,rh2} = P'^{rh2,d}_{t,d} + P'^{rh2,shht}_{t,d} \quad \forall t \epsilon T, d \epsilon D \tag{eq. 103}$$

$$P'_{t,d,pth} = P'^{pth,sh}_{t,d} + P'^{pth,d}_{t,d} \quad \forall t \epsilon T, d \epsilon D \tag{eq. 104}$$

$$P'_{t,d,ptg} = P'^{ptg,sf}_{t,d} + P'^{ptg,d}_{t,d} \quad \forall t \epsilon T, d \epsilon D \tag{eq. 105}$$

$$P'^{load}_{t,d,sh} = P'^{rh1,sh}_{t,d} + P'^{pth,sh}_{t,d} \quad \forall t \epsilon T, d \epsilon D \tag{eq. 106}$$

$$P'^{unload}_{t,d,shht} = P'^{shht,d}_{t,d} + P'^{shht,htp}_{t,d} \quad \forall t \epsilon T, d \epsilon D \tag{eq. 107}$$

$$P'^{unload}_{t,d,sf} = P'^{sf,gtp}_{t,d} + P'^{sf,d}_{t,d} \quad \forall t \epsilon T, d \epsilon D \tag{eq. 108}$$

Energy shortage measurement

$$ESh^{e}_{t} = \sum_{d} Demand^{e}_{t,d} - \left(P'_{t,d,r1} + P'_{t,d,r2} + P'_{t,d,htp} - \frac{P'_{t,d,pth}}{\eta_{pth}} + P'_{t,d,gtp} - \frac{P'_{t,d,ptg}}{\eta_{ptg}} - P'^{load}_{t,d,se} + P'^{unload}_{t,d,se} \right) \quad \forall t \epsilon T \tag{eq. 109}$$

$$ESh^{h}_{t} = \sum_{d} Demand^{h}_{t,d} - \left(P'_{t,d,rh1} + P'_{t,d,rh2} + P'^{pth,d}_{t,d} + P'^{shht,d}_{t,d} + P'^{unload}_{t,d,sh} \right) \quad \forall t \epsilon T \tag{eq. 110}$$

$$ESh_t^f = \sum_d Demand_{t,d}^f - \left(P'^{ptg,d}_{t,d} + P'^{sf,d}_{t,d}\right) \quad \forall t \epsilon T \tag{eq. 111}$$

$$ESh_t^{+e} \geq ESh_t^e \quad \forall t \epsilon T \tag{eq. 112}$$

$$ESh_t^{+h} \geq ESh_t^h \quad \forall t \epsilon T \tag{eq. 113}$$

$$ESh_t^{+f} \geq ESh_t^f \quad \forall t \epsilon T \tag{eq. 114}$$

Resilience indicator

$$Re^e = 1 - \frac{\sum_t ESh_t^{+e}}{Demand^e} \tag{eq. 115}$$

$$Re^h = 1 - \frac{\sum_t ESh_t^{+h}}{Demand^h} \tag{eq. 116}$$

$$Re^f = 1 - \frac{\sum_t ESh_t^{+f}}{Demand^f} \tag{eq. 117}$$

$$Re^{total} = \frac{Re^e \cdot Demand^e + Re^h \cdot Demand^h + Re^f \cdot Demand^f}{Demand^{total}} \tag{eq. 118}$$

ε-constraint equation

$$Re^{total} \geq Re^{max} - (1 - \omega_{Re}) \cdot \left(Re^{max} - Re^{min}\right) \tag{eq. 119}$$

Objective function

$$\min Costs^{total} \tag{eq. 120}$$

H. Appendix H: Inputs for the Model

The inputs of the model are available in the next link: https://cutt.ly/0rxkgyI.

The link references an Excel spreadsheet. The worksheet “Scenarios” configure the different scenarios to be used as the model type, the relative weight of the OFs, the time event, the time horizon and the PGA. The worksheet “Inputs” summarizes all the inputs for the model, whose are referenced in the same spreadsheet.

I. Appendix I: GAMS Model

The complete model is available in the next link: https://cutt.ly/jrxkhvY .

The link references a GAMS code. It calls the abovementioned Excel spreadsheet from Appendix H and uses the data as input for the model.